Accelerator Department
BROOKHAVEN NATIONAL LABORATORY
Associated Universities, Inc.

EP&S DIVISION TECHNICAL NOTE

No. 88

P. Yamin

July 20, 1979

THE ISA DETECTOR TEST FACILITY

A facility for testing detectors to be used at ISABELLE will be constructed at the AGS. During the fall of 1979 the MESB/B4 will be used temporarily, but in early 1980 the B1 line will become available. There are no other commitments or pending proposals for the B1 beam, so it can be devoted to the Detector Test Facility (DTF) indefinitely. As both B1 and B4 service adjacent areas on the AGS floor, a compact layout encompassing both beams is envisioned for late 1981. This is illustrated in Figure 1.

The MESB/B4 provides separated πs, Ks, ps, and $\bar{p}$s at moderate intensities between 1 and 10 GeV/c. B1 is an unseparated 0° production-angle beam which can deliver high fluxes ($\sim 10^{7}$/sec) up to 24 GeV/c. Thus, the DTF will be able to simulate many of the features of the ISABELLE environment. Fig. 2(a-f) shows the particle fluxes available in these beams.

The DTF will be arranged so that tests can be conducted expeditiously. A counting house-trailer will contain a PDP11/60 and will be supplied with NIM and CAMAC electronics from HEEP. Crane coverage is unobstructed, and the area is free of encumbrances. Sufficient water and power will be provided to operate one large spectrometer magnet, and provision will be made for the eventual installation of cryogenic services, should it prove necessary.

Operating instructions and other details are given in the appendices. Appendix I is a report by C.T. Murphy and J. Fox describing the MESB and Appendix II gives more information about B1 than is available elsewhere.

List of Figures

1. DTF Layout.
2. Fluxes Available in the MESB and B1.

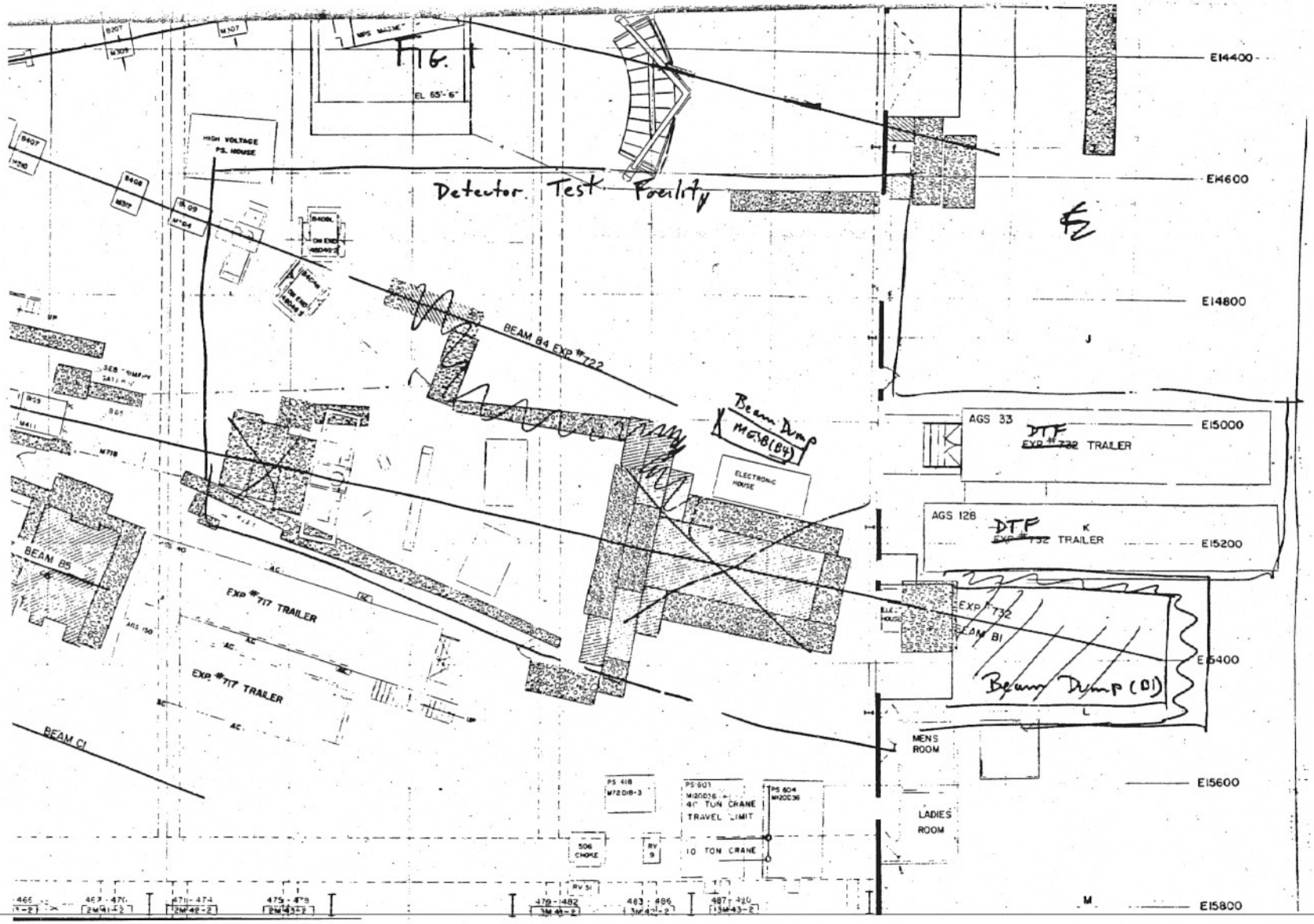
Fig. 1
Detector Test Facility
EL 65'-6"
HIGH VOLTAGE P.S. HOUSE
BEAM B4 EXP #722
Beam Dump M6(B4)
ELECTRONIC HOUSE
BEAM B5
Exp #717 TRAILER
Exp #717 TRAILER
BEAM C1
AGS 33
DTF
EXP #732 TRAILER
AGS 128
DTF
EXP #732 TRAILER
K
Exp #732
BEAM B1
Beam Dump (D1)
MENS ROOM
LADIES ROOM
PS 418
PS 601
40' TUN CRANE
TRAVEL LIMIT
PS 604
506 CHOKE
10 TON CRANE
E14400
E14600
E14800
J
E15000
E15200
E15400
E15600
M
E15800

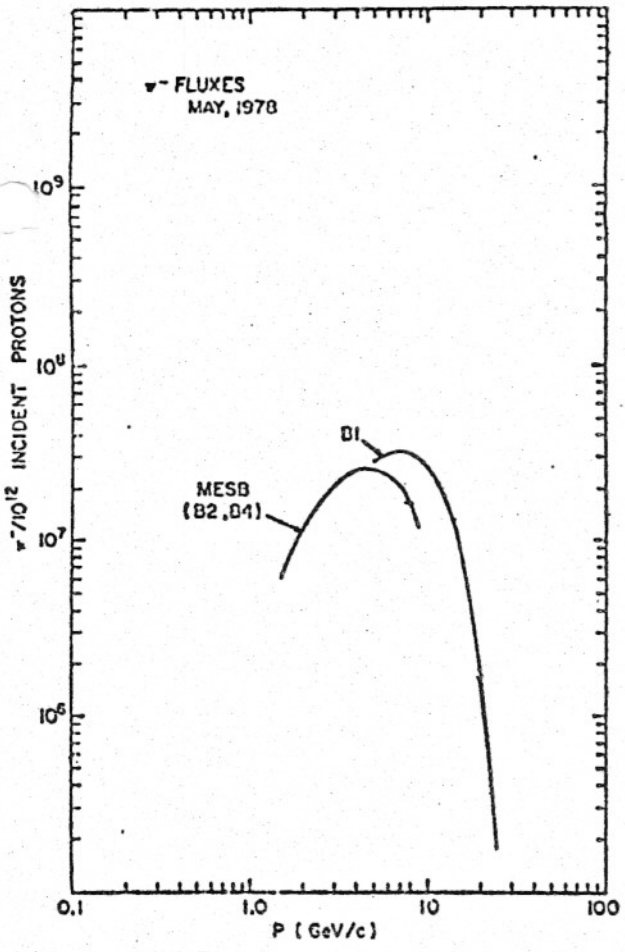
π⁻ FLUXES
MAY, 1978
π⁻/10¹² INCIDENT PROTONS
BI
MESB
(B2,B4)
P (GeV/c)

(a)

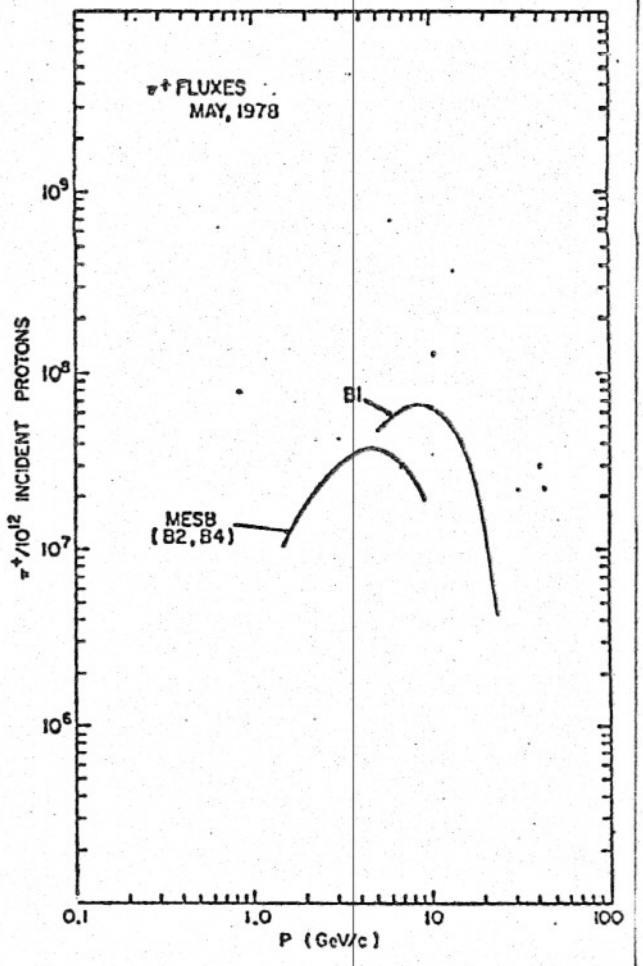
π⁺ FLUXES
MAY, 1978
π⁺/10¹² INCIDENT PROTONS
BI
MESB
(B2,B4)
P (GeV/c)

(b)

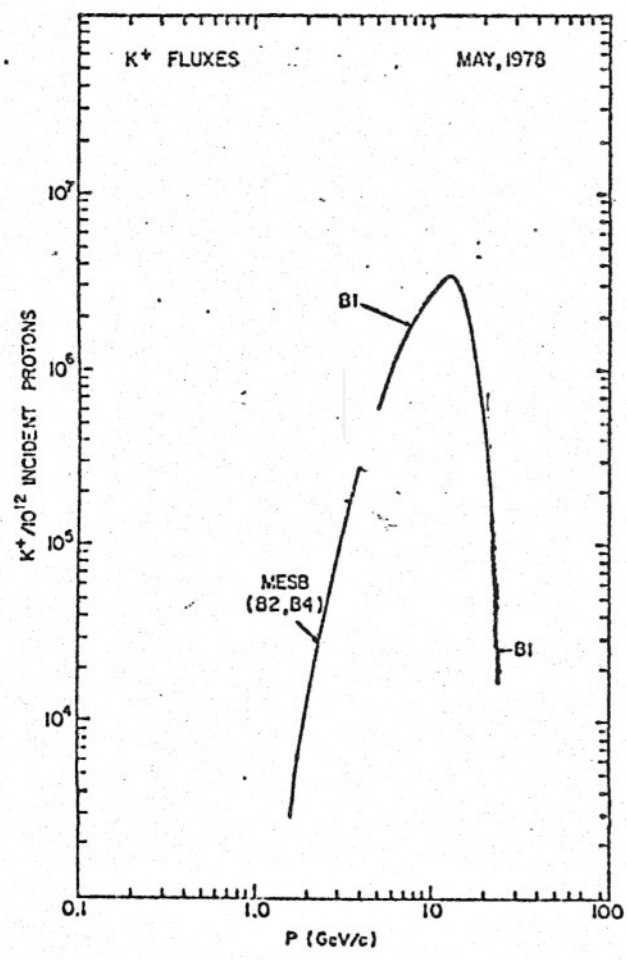
K⁺ FLUXES
MAY, 1978
K⁺/10¹² INCIDENT PROTONS
BI
MESB
(B2,B4)
BI
P (GeV/c)

(c)

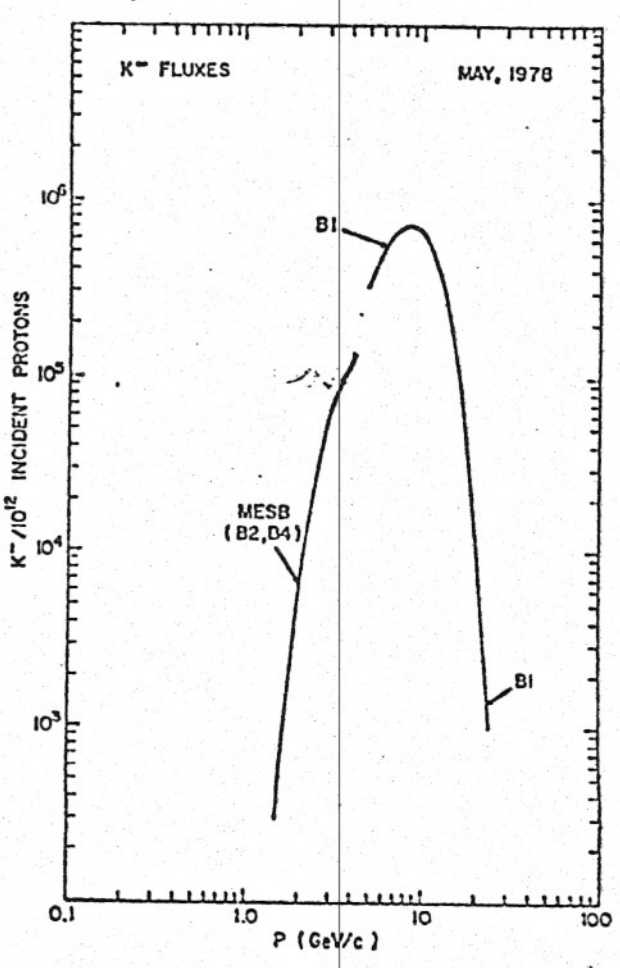
K⁻ FLUXES
MAY, 1978
K⁻/10¹² INCIDENT PROTONS
BI
MESB
(B2,B4)
BI
P (GeV/c)

(d)

Fig. 2 (a-d)

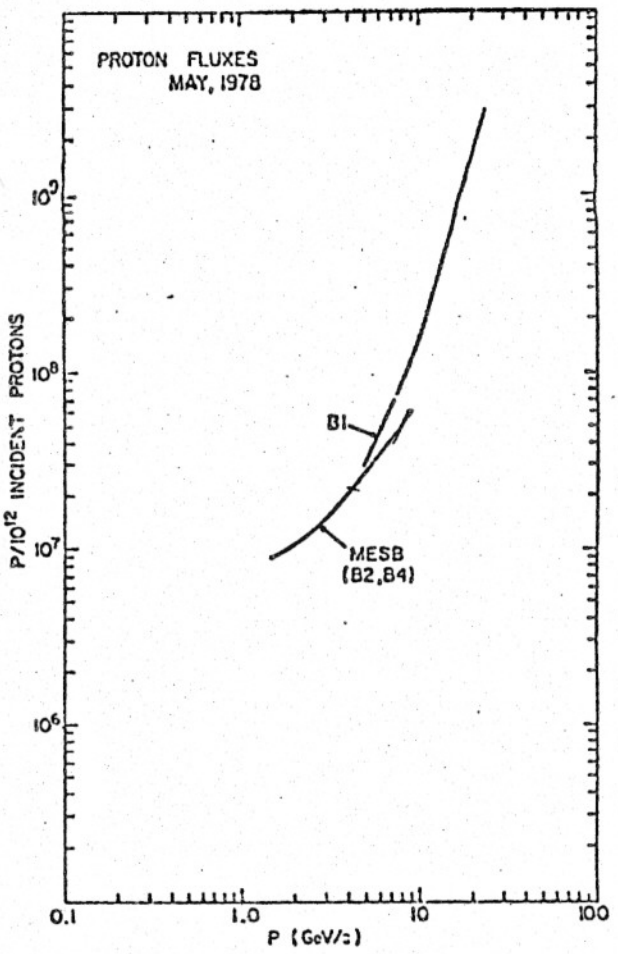
PROTON FLUXES
MAY, 1978
B1
MESB
(B2,B4)
P/10^12 INCIDENT PROTONS
P (GeV/c)
0.1
1.0
10
100

(e)

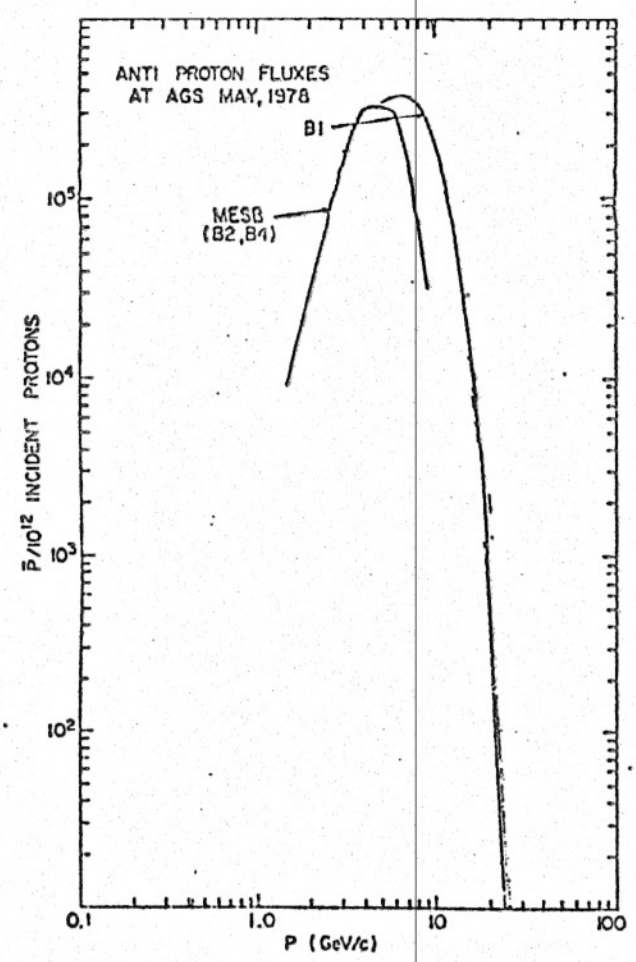
ANTI PROTON FLUXES
AT AGS MAY, 1978
B1
MESB
(B2,B4)
P/10^12 INCIDENT PROTONS
P (GeV/c)
0.1
1.0
10
100

(f)

Fig. 2 (e-f)

BNL 18627

BROOKHAVEN NATIONAL LABORATORY
Associated Universities, Inc.
Upton, New York

ACCELERATOR DEPARTMENT
Informal Report

CHARACTERISTICS OF MESB: DESCRIPTION FOR USERS

C.T. Murphy* and J.D. Fox+
January 28, 1974

* Present Address: National Accelerator Laboratory, Batavia, Illinois

\+ Present Address: Saclay, Centre d'Etude Nucleaire de Saclay, France

ABSTRACT

The beam optical design and calculated performance data are presented for the Medium Energy Separated Beam from the "B" target station. Various modes of operation which enable the beam to separate kaons to 6 GeV/c, and anti-protons to 9 GeV/c are discussed. Purified particle fluxes in excess of 10^5 K^+, 5×10^4 K^-, and 10^5 $\bar{p}$ per 10^{12} protons interacting in a beryllium target are anticipated.

N O T I C E

This report was prepared as an account of work sponsored by the United States Government. Neither the United States nor the United States Atomic Energy Commission, nor any of their employees, nor any of their contractors, subcontractors, or their employees, makes any warranty, express or implied, or assumes any legal liability or responsibility for the accuracy, completeness or usefulness of any information, apparatus, product or process disclosed, or represents that its use would not infringe privately owned rights.

Introduction

The Medium Energy Separated Beam (MESB) is a one-stage, DC separated beam from the AGS external proton beam target B, designed to purify K's up to 6.0 GeV/c and $\bar{p}$'s up to 9.3 GeV/c for electronic experiments. The momentum limit is determined by the measured $\int Bdl$ of the first bending magnet at full current.

MESB was originally designed by Carroll[1] to separate 5 GeV/c K's and 8 GeV/c $\bar{p}$'s. Fox[2] increased the upstream bend angle in order that the beam reach the MPS (multiparticle spectrometer), added a quadrupole to the front-end doublet so as to approximately double the low momentum flux, and arranged a Y branch in the downstream end. This third effort on the beam design has resulted in a full utilization of the variable-focal length properties of the front-end triplet so as to increase the momentum-limit of separability.

Some details remain to be studied -- most notably, the optimum target material and length, multiple scattering in the Cerenkov counters, beam instrumentation and how to tune the beam, and muon contamination. Hence both the flux and the remaining contamination are somewhat uncertain: only lower limits can be set on both. What is firm is the position and number of elements in the beam, which have been determined by the sometimes conflicting requirements of momentum recombination and adequate K-π separation in both branches and the several modes of the beam. In addition, the placement of the final two quadrupoles in each branch of the beam is regarded as experiment-dependent and has been studied only for 5 approved experiments. It is the responsibility of each experimental group to decide on the placement of the last two quadrupoles and the position of the first horizontal focus.

The purpose of this note is to familiarize potential users with the certain aspects of the beam and invite participation and assistance in the resolution of the uncertain details of the tail end of the beam. First, the beam optics are discussed in a cursory fashion; then probable fluxes, purity, and spot sizes (or phase spaces) at the final focus of the beam are discussed.*

Layout

The layout of the beam is shown in Fig. 1. At the upstream end, the beam accepts particles at a 6° production angle from a target shared simultaneously with the 0° unseparated beam. At the downstream end, the beam serves experiments non-simultaneously at two places: (a) the East branch, in the region between MPS and the 0° experiments; (b) the West branch, or MPS. These branches are hereafter abbreviated E and MPS (or W).

Variable Focal Length Front Triplet: Modes 1-3

The variable-focal length triplet, Q1-2-3, allows the K-π separation at the first vertical focus (the mass slit) to be held constant at twice the magnified, unaberrated, target height (a condition referred to hereafter as "$\eta = 2$") as the momentum is increased, in a continuous manner. As the momentum increases, the vertical focal length (f_v) increases and

---

*More detailed documentation on the beam exists in the form of EP&S Technical Notes: MESB Design Notes, referred to here just as Design Note:

I. Tolerances on the Uniformity of $\int Bdl$ in D1 and D2 (EP&S No. 59).
II. Mass Slit Operation and Pion Contamination (EP&S No. 62).
III. The Midsection: Variable Position of Horizontal Focus, Two Sextupoles, and Vertical Chromatic Aberration.
IV. Annotated BEAM Output and Input.

the vertical acceptance angle (y'_t) decreases, in proportion. However, there are upper and lower limits in this variation. The lower limit, designated as mode 1 of the beam, occurs when Q3 is horizontally filled to its maximum usable aperture of about 5.5". The optics of this mode are illustrated in Fig. 2, for the first half of the beam. In this mode, f_v = 270", y'_t = 3.7 mrad, and the beam separates with $\eta \geq 2$ up to 4 GeV/c K's and 6.3 GeV/c $\bar{p}$'s. This mode is a lower limit because lowering the vertical focal length any further leads to greater losses in horizontal acceptance angle than gains in vertical acceptance angle. Hence experiments below 4 GeV/c can do no better than to run in mode 1. The upper limit, designated as mode 3, has the polarities of Q2 and Q3 reversed from those of mode 1 and is defined as the point at which the vertical focal length is a maximum (850"). The optics are shown in Fig. 3. This mode separates 6 GeV/c K's and 9.4 GeV/c $\bar{p}$'s with η = 2. The gradients in the triplet are shown as a function of momentum (as the focal length is gradually increased to 850") in Fig. 7.*

Table I lists the properties of the beam up to the mass slit for modes 1, 3 and 4 (mode 4 is explained later) in the East and West branches. Gradients and bending magnet fields are listed in Table II for 5 GeV/c only. For exact information on modes in between 1 and 3, a beam program such as BEAM must be run. Alternately, the following crude scaling can be applied: the solid angle decreases proportional to P^{-3}; bending magnet fields and quadrupole gradients (excepting Q1-2-3) increase linearly with P, except

---

*Mode 2 is the point where the gradient of Q3 is zero. The mountain in the current required by Q1 as one moves continuously from mode 1 to mode 3 has been named after the physicist who first objected to the excessive power requirement of that mode. It is probable that the power supply initially assigned to Q1 will not permit running near mode 2.

for Q6, which is both mode and branch dependent. In the East branch the Q6 gradient increases as P^2; in the West branch, the gradient remains roughly constant.

Dispersion and Separation

The bending magnet D1 disperses the beam in the horizontal plane. Following Q3, four rectangular separators, assumed to operate at 225 kV/inch, separate K's from π's in the vertical plane. The physical separation is achieved in the mass slit at the first vertical focus. A sextupole placed near the first horizontal focus (just after Q4) corrects most of the chromatic aberration in the vertical plane at the mass slit. The momentum bite of the beam is defined by a remotely variable collimator just downstream of the first sextupole.

As can be seen in Figs. 2 and 3, mode 3 will barely transmit a momentum bite of $\pm$ 2.5% through Q4, while mode 1 could transmit $\pm$ 5%. However, K-π separation is aberration-limited with a bite of $\pm$ 3% in mode 1, at least at 4 GeV/c where $\eta = 2$. At lower momenta, it might be possible to separate a bigger momentum bite.

Midsection

The midsection of the beam (Q4, Q5, D2, Q6, D3, D4) focuses vertically at the mass slit, recombines momenta in both angle and position and achieves the desired beam size at the entrance to the final doublet (experiment dependent). The optics differ immensely in the two branches and change from mode to mode. The following sketch is amplified in Design Note III.

D2 steers the beam towards D4 which switches the beam either to the MPS or to the open area between MPS and the 0° beam experiments. D2 and D4 alone would not quite get a 9.3 GeV/c beam to MPS, so D3 was added and put directly behind the mass slit in order to also sweep out low-energy particles produced in the mass slit. A sufficient drift space was necessary between D3 and D4 to allow D4 to be part of a beam spectrometer for momentum determination.

To first order, each of the three quadrupoles has a single function. Q4 is a field lens for off-momentum particles and steers them into D2-3-4 such that they emerge with the same angles an on-momentum particles. Q5 focuses vertically on the mass slit. Q6 centers off-momentum particles in D4 such that they emerge position-recombined. In the West leg, this requirement results in Q6 forming a nearly parallel beam (for on-momentum particles); in the East leg, the "unnatural" direction of the D4 bend requires that Q6 make an extra horizontal focus somewhat in front of D4. Therefore Q6 requires much more gradient in the East leg modes than in the West leg. Because of very strong second-order mixing of the functions of the quadrupoles, the gradients in Q4 and Q5 are also much larger in the East branch than in the West.

Control over the size of the beam at the entrance to the final doublet (or triplet) which focuses the beam on the experimental target is provided by allowing the position of the first horizontal focus to be variable. This flexibility is necessary in order to obtain downstream optics which are independent of mode (momentum). In most modes it was found that if the position of the first horizontal focus was the sextupole immediately following Q5, then the beam, tuned to be momentum recombined in both

position and angle, would enter the final doublet with a size roughly filling the first quadrupole of the doublet. However, in mode 1W, momentum recombination demanded that the next horizontal focus occur at the entrance of the final doublet, leading to a beam size at the experimental target which was very large. By moving the first horizontal focus 65" downstream, the downstream horizontal optics became roughly the same as in Mode 3W.

The general rule of thumb is the following: to make the beam bigger (horizontally) at the final doublet, move the first horizontal focus downstream.*

Moving the horizontal focus further downstream than the second sextupole (1753" from B target) brings about rapidly increasing beam losses on the 12" aperture of Q4, and is thus not recommended.

Correction of vertical chromatic aberrations with sextupoles still works even if the horizontal focus is not exactly at a sextupole. In the region between Q5 and D2, the beam is going out of focus so slowly that one can do just as good a job with the nearest sextupole as one would do with a sextupole exactly at the focus. If the focus is moved upstream of Q5 (as in East modes), it is advisable to get an extra power supply and power both sextupoles, one negative and one positive, in a ratio given in Design Note III. Numerical data supporting this paragraph also appear in that Note. The position of the first horizontal focus is a variable which the user can control and change.

*In Mode E1, there is a problem with scraping in Q6. It was found that this was relieved somewhat by moving the first horizontal focus upstream to the end of Q4. (Mode E3 has a scraping problem in the final doublet, which could probably be relieved by moving the first focus up to the end of Q4.)

Purity of Separation and Aberrations

The condition $\eta = 2$ which we have selected as a minimum condition of separability means that the center of the pions is separated from the center of the kaons at the mass slit by a distance of twice the geometrical image height, i.e., target height times magnification. If there were no aberrations, one could separate with $\eta = 1$. However, chromatic aberrations alone more than double the image widths, so that the K and π images are very overlapped in some modes.

The sextupole at the first horizontal focus would remove the chromatic aberration entirely if the width of the horizontal image (for a given momentum) were zero. However, the target appears to be very wide, specifically, the length (4") times sin6°, which is 0.42", so that at the first horizontal focus the image of on-momentum particles touches the edge of the image of particles with $\Delta P/P = 2.5\%$. The result is that the sextupole removes only about half of the chromatic aberration. The K's and π's remain overlapped.

A mass slit has been designed which intercepts π's in the overlapped region of phase space (at the expense of intercepting up to 22% of the K's), and is fully documented in Design Note II. In summary, that Note shows that with the criterion of $\eta = 2$ (which defines the highest momentum at which modes 1 and 3 can be used) the π/K ratio at the experiment is predicted to be between 0.26 (Mode 1E) and 1.80 (Mode 3E). These are lower limits because no other aberrations have been quantitatively studied (except the sextupole component of D1 -- see Design Note I and Figs. 12 and 13 of this document).

Other potential aberrations are separator non-uniformity or instability, quadrupole aberrations, and scattering from magnets and the momentum

collimator in the region between the separators and the mass slit. Undocumented hand calculations indicated that separator and quadrupole aberrations were insignificant. The scattering problem has been given no thought.

Purity can always be improved, of course, by running in a mode in which $\eta > 2$, e.g., using Mode 3 for 5 GeV K^-.

Moving Q6 for Mode 3E

It was found that most of the chromatic aberration in Mode 3 (East or West) came from the Q4-5-6 triplet. In Mode 3E (and only Mode 3E) it was found that a significant reduction in the π/K ratio was achieved by moving Q6 downstream by 150" from its normal position (moving it further downstream pushed the gradient too high). The reduction in the π/K ratio was roughly a factor of 2. Data quoted for Mode 3E assume this change. However, it seems prudent to verify experimentally this improvement before accepting such a rerigging problem as part of the demands of experiments in the East leg.

Mode 4

Chromatic aberration is reduced by a factor of 2 at the mass slit by reversing the polarity of Q4-5, as explained in Design Note III. However, off momentum particles with $\Delta p/p \geq 1.5\%$ are then lost in Q4, so the total flux is reduced. This mode is as pure in π/K ratio at 6.6 GeV as Mode 3 is at 6 GeV/c, in our computer idealization, so that this mode might extend the usable momentum range of the beam for kaons up to 6.6 GeV/c. Alternately, this mode is a safety valve for approved experiments at 6 GeV, should the K/π ratio prove to be intolerable in Mode 3.

Downstream Optics

The position of the final focusing elements is the responsibility of the user. However, a number of arrangements for approved experiments have been studied and are presented as examples. The properties of the beam at the final focus for these examples are shown in Table III.

The spot sizes shown in Table III include chromatic aberration only, and do not include the important effect of multiple scattering in the beam Cerenkov counters, an effect which is both momentum and experiment dependent (see below).

In the East leg D. O'Brien selected the positions for D4, Q7 and Q8 and decided to leave D3 off in order not to place the experimental area too close to the 0° beam experiments.*

The final focus in Mode 3 of the West leg has been studied for three arrangements of the final focusing elements. The first, called 3WCRAM tries to cram the beam into a small 12" target. The width, ΔX, is small and the divergence ($\Delta X'$) is large. The spacing of Q7-8 is quite large. Mode 1W has been studied only for the CRAM conditions (Column 1, Table III).

The mode called 3WCMU is the arrangement created for the CMU experiment, which wanted a spot which would fit inside a 3" LH2 target in front of the MPS magnet but would be reasonably small in a beam anti-counter 385" downstream of the LH2 target. The vertical focus is actually 240" downstream of the LH2 target. The size of the beam at the anti-counter (100% of particles, but no multiple scattering) is 6" x 1.7".

---

*Extensive studies of this leg were written by O'Brien. We disagree with his estimates of K:π ratio (see Design Note II) and find no mention of the serious (25%) scraping problem in Mode 3E (see Table III, last row). This scraping problem might be cured by moving the first horizontal focus upstream of its current position (1623") or by moving Q7-8 upstream.

The mode called 3WROT uses a triplet, rotated 45° from the normal orientation, to perform an imperfect interchange (or rotation) of the x and y phase spaces. The details are the subject of a separate note (Design Note IV). This rotation is desirable for experiments which need a small horizontal phase space.

In principle, the horizontal phase space ($\Delta X\ \Delta X'$) and vertical phase space ($\Delta y\ \Delta y'$) should be the same in all modes (Liouville's theorem). Excepting mode 3WCRAM, the theorem holds within 20% for the horizontal plane but only within a factor of 4 for the vertical plane. The variations result from differing amounts of chromatic aberration in the various modes. The phase spaces in Mode 4 are smaller since the momentum bite is only $\pm$ 1.5%; the horizontal phase spaces in the East leg are bigger because of the increased focusing necessary in order to have three horizontal foci.

Perfect interchange of phase space in Mode 3WROT would result in a vertical phase space of $\sim$24 mr-inches and a horizontal phase space of $\sim$1 mr-inch. In fact the two numbers turn out to be 29 mr-inches and 4.4 mr-inches. The factor of 4 increase in the horizontal phase space comes half from the increased chromatic aberration of the triplet and half from the fact that it takes at least four quadrupoles to do an exact rotation.

Fitting four quadrupoles into the line, with spacings adequate to keep gradients low enough, was proven impossible. In order to perform the imperfect interchange documented here, using the two 12Q30's assigned to MESB plus a borrowed 8Q48, the spacings had to be lengthened such that the beam momentum spectrometer arm following D4 is shortened by a couple of feet in order to keep gradients low enough that 9.3 GeV/c is achieveable.

Multiple Scattering in the Beam Cerenkov Counters

Three threshold beam Cerenkov chambers are being built by CMU, two of which distinguish π's from K's, one of which distinguishes K's from p's (or $\bar{p}$'s). The gas will be ethane.

Edelstein[4] has calculated that the K-p counter, operating at 270 psi at 3 GeV/c, will cause 2 mr (not projected) of multiple scattering (rms). This number is large compared to the natural divergence of the vertical plane (2 mr) in most modes, and so could cause a very large broadening of the image. This problem has been discovered only recently and has not been studied carefully. The remainder of this section gives sufficient information so that the user can calculate the effect for his experiment, and select Cerenkov positions which minimize the effect.

The multiple scattering is very momentum dependent. In the simple assumption that the counter is actually operating at threshold, the mean multiple scattering angle is proportional to m/p^2, where m is the mass of the particle and p is the momentum. The windows on the counter are the dominant source of scattering at high momenta. At 3 GeV, using kaons, there are 2 mr multiple scattering in the gas and 1.1 mr in the window. At 6 GeV/c there is 0.6 mrad multiple scattering in both the gas and the windows.

To translate mean multiple scattering angles into mean broadening at the final focus is trivial for a Cerenkov counter in the drift space preceding the final focus. For counters upstream of the last quadrupole the calculation requires a well-known theorem from beam optics. If a scattering, $\delta\theta_p$, occurs in the vertical plane at some point P along the beam, then the deviation in y of the ray traced back to the target, δy_t, is given by

$$\delta y_t = b_p \, \delta\theta_p$$

where b_p is the (1,2) matrix element in the transfer matrix relating rays at the target to rays at p:

$$\begin{pmatrix} y_p \\ y'_p \end{pmatrix} = \begin{pmatrix} a_p & b_p \\ L_p & d_p \end{pmatrix} \begin{pmatrix} y_t \\ y'_t \end{pmatrix}$$

The value of b_p at any point along the beam can be calculated for any mode from the paraxial ($y_t = 0$) ray traces of Figs. 2-6:

$$b_p = \frac{y_p}{y'_t}$$

where $y'_t = 0.00368$ rad for mode 1 and 0.00115 rad for mode 3. The deviation at the final focus is simply δy_t times the vertical magnification given in Table III:

$$\delta y_f = m_v \frac{y_p}{y'_t} \delta\theta_p \qquad (2)$$

For example, suppose there is an rms multiple scattering of $\pm$ 1 mr in the vertical plane in a Cerenkov counter placed just behind Q7 in mode 3WCRAM, where $y_p \simeq 1"$. Then

$$\delta y_f = \pm \frac{(0.75)(1)(.001)}{(.00115)} = \pm\ 0.65"$$

This is large compared to the predicted final spot size of 0.2".

The same theorem applies to the horizontal plane but leads to less disastrous broadening because $x'_t = 20$ mr. To minimize multiple scattering the K-p Cerenkov counter should be placed at a place where y_p (or x_p) is small, i.e., near a focus. Some users may wish to put one of the Cerenkov counters behind D3, at the cost of shortening the beam spectrometer.

It is not clear how to do the calculation for mode 3WROT in which the vertical and horizontal planes are mixed.*

Intermediate Modes and Program BEAM

Up-to-date output for modes between 1 and 3 do not exist. During the design, mode 2 was occasionally run and seemed to have no problems.

The simplest way to obtain output for intermediate modes is to use the program BEAM because self-tuning input decks already exist. The program and input decks can be obtained from the EP&S group. One simply changes the value of Q1, using Fig. 7; input cards in the deck then tune all other quadrupoles, demanding foci in the correct places and momentum recombination in angle and momentum. If the change in the value of Q1 is large, the focusing routines may not converge; in that case several runs need to be made, moving Q1 in steps towards the desired value and inserting the latest set of quadrupole gradients for each run.

Program BEAM has the disadvantage that there is no documentation other than Design Note V. Comment cards are fairly generous however.

Target Design

The properties of the beam listed in Table I assumed a target of dimensions (height, width, length) = (0.04", 0.10", 4"). It is hoped that it can be shaped as shown below.

---

*Program BEAM has an input card reserved for multiple scattering elements; however, this branch of the program is now inoperative. Comment cards in subroutine TRACE indicate how to reinstitute the branch.

Conservative estimates of fluxes have been made using the data on production in beryllium of Sanford and Wang.[3] Extrapolations to heavier nuclei are uncertain because of reabsorption in the struck nucleus. It is estimated that for K^- perhaps a gain of a factor 2 (per inch of target length) can be achieved using copper instead. The optimization problem has yet to be studied in detail, and is probably experiment dependent. In addition, the target must satisfy the requirements of the 0° beam.

Target Plan View (not to scale)

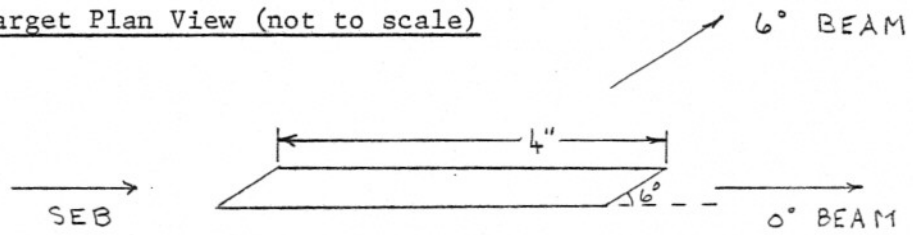

At the moment, 5 targets have been designated to be available on the target table: 4" Be, 2" Be, 4" Cu, 2" Cu, and 2" W. All will be shaped as shown above.

Fluxes

Fluxes can be calculated with the aid of Figs. 8-10, which give yields at the final foci per 10^{12} interacting protons in beryllium at 6° (phase I) and 3° (phase II). The dotted curves show the yields in modes 1 and 3 assuming the full solid angles and momentum bites of Table I; the solid curves show the yield as one gradually varies the focal length of the front triplet, moving continuously from mode 1 to

mode 3. For $K^{\pm}$ above 6 GeV, mode 4 is shown. Otherwise, the curves include the effect of 70% transmission of the full solid angle and momentum bite through MESB, a figure resulting from Monte Carlo studies.

To obtain the true flux in the beam, one must fold in the number of protons in the external beam and the fraction which interact in the target. If 4" of beryllium is used, this fraction might be 1/6, assuming that all protons hit the target. It is hoped that this estimate is conservative.

Approximately the same results were obtained by O'Brien using Hagedorn-Ranft particle production curves.

Momentum Bite

The momentum bite in the MESB will not be very sharply defined because of the very large effective target width. At the momentum collimator, the image of on-momentum particles touches the edge of the image of particles with $\Delta P/P = 2.5\%$. Fig. 14 shows the momentum spectra expected in modes 1 and 3 when the momentum collimator is set at the center of the image of particles with $\Delta P/P = \pm 3.0$ and 2.5%, respectively. The rule-of-thumb is that the momentum distribution always extends 1% beyond the desired bite.

The momentum bite is slightly more sharply defined for mode 1W than for 1E, as a result of the fact that the horizontal focus for mode 1E is not at the collimator but upstream of Q5.

Momentum Determination

In the West leg, a beam spectrometer of proportional wire chambers around D4 will determine the momentum of individual particles to $\pm$ 0.25%. An independent spectrometer is planned for the East leg.

Beam Size at Various Magnets

For guidance in designing detection devices, Table IV gives the spot size of the beam (100% of the particles) at various points along the beam.

Collimators

A remotely variable horizontal collimator follows Q1. A fixed aperture (2") collimator is planned to be inserted in Q3. To degrade muons and stop secondaries from the mass slit, D3 has a vertical aperture of 1.25 inches. A remotely variable horizontal collimator just after the first sextupole determines the momentum bite. Both remotely variable horizontal collimators have separate drives for the right and left plate. Both are made of heavimet.

In mode 3E the mass slit is also a horizontal focus, so the mass slit should be followed by a horizontal stop which can be crude, as it will be in air. The corresponding horizontal focus in mode 1E is just in front of D4, where it would be desirable to have the possibility of a horizontal collimator. However, none is planned.

The square pipe through the steel proton beam shield wall in the middle of the separators is a natural vertical collimator. It would be wise to put a fixed aperture horizontal collimator inside Q4 in order to remove very off-momentum particles from the bad-field region of Q4. These

off-momentum particles will not necessarily be removed by the momentum collimator.

Phase II

The layout as shown is called phase I. It is actually not very usable above 7 GeV for $\bar{p}$'s, as the flux at a 6° production angle is falling very fast (see Fig. 10). Hence a phase II of the MESB is envisaged in which a septum bending magnet is added in front of Q1 which will bend particles produced at 3° towards the fixed bend point of D3; Q1 and Q2 are moved inward a few inches. The rest of the beam remains intact and then will transport up to 9.3 GeV/c, limited entirely by D1. The $\bar{p}$ flux should increase by a factor of 3 at 7 GeV/c and a factor 6 at 10 GeV/c. Phase II also has the fringe benefit of reducing two problems associated with the large apparent width of a 4" long target viewed at 6°. This large apparent width creates a rather large horizontal phase space, so that small spot sizes are difficult to achieve. Secondly, this large width induces large aberrations in the vertical plane in mode 3 at the mass slit, making separation very marginal. In phase I, the only cures available, such as halving the target length, result in a loss of flux. With a 4" target in phase II (3° production), both the vertical plane aberrations and the horizontal spot size are dominated by other effects (largely chromatic aberration).

Acknowledgements

Useful suggestions and criticisms have been received from D. Berley, H. Brown, A. Carroll, and H. Foelsche. The program used was written by J. Fox. E. Makuchowski provided much assistance in altering and executing the computer program. E. Willen edited the final draft and the figures.

B1, B2 Distribution

References

1. A. Carroll, Summer Study on AGS Utilization, 1970.

2. J.D. Fox, EP&S Division Technical Note No. 38, 1970.

3. J. Sanford and C.L. Wang, AGS Internal Report, 1967.

4. Note on Beam Cerenkov Counters for MESB/MPS, R.M. Edelstein, May 1973.

TABLE I - Properties of MESB Phase [illegible] Production) up to the Mass Slit

Definitions:

$\eta_K \equiv \frac{\text{K-}\pi \text{ separation at mass slit}}{\text{magnified geometrical target height}}$

$\theta_V \equiv$ vertical plane divergence

$\theta_H \equiv$ horizontal plane divergence

Front End	Mode 1	Mode 3	Mode 4
Max. θ_V	± 3.68 mr	± 1.15 mr	± 1.15 mr
Max. θ_H	± 20 mr	± 20 mr	± 20 mr
Ω (geometrical solid angle) = $4\theta_V\theta_H$	294 μst	92 μst	92 μst
Assumed production target (height x width x length)	.04" x 0.10" x 4"	.04" x 0.10" x 4"	.04" x 0.10" x 4"
f_v (vertical front focal length)	274"	860"	860"
momentum at which $\eta_K = 2$	4.0 GeV/c	6.0 GeV/c	6.6 GeV/c (η=1.5)≠
momentum at which $\eta_{\bar{p}} = 2$	6.3 GeV/c	9.4 GeV/c	9.4 GeV/c

At first horizontal focus	1W	3W CRAM	3W CMU	3W ROT	4W	1E	3E	4E
distance from target	1688"	1623"	1753"	1753"	1623"	1517"	1623"	1545"
± ΔP/P (max. momentum bite)	± 3.0%*	± 2.5	± 2.5	± 2.5	± 1.5	± 3.0%*	± 2.5	± 1.5
dispersion at momentum collimator†	0.89"/%	1.27"/%	1.20"/%	1.08"/%	2.46"/%	1.00"/%	1.78"/%	2.54"/%
horizontal magnification	3.2	6.3	5.7	5.5	13.0	3.6	4.8	12.6
horizontal image full width (on momentum)	1.34"	2.62"	2.24"	2.32"	5.52"	1.50"	2.0"	5.3"
At mass slit								
distance from target	2152"	2152"	2152"	2152"	2152"	2152"	2152"	2152"
vertical magnification	2.41	0.63	0.65	0.59	1.00	2.3	0.58	1.40
K-π separation at momentum where η = 2	0.194"	0.050"	0.054"	0.047"	0.060"≠	0.184"	0.046"	0.084"≠
max. θ_V	±1.52mr	±1.83mr	±1.77mr	±1.95mr	±1.15mr	±1.60mr	±2.00mr	±0.82mr
horizontal full width	6.0"	6.0"	5.4"	5.4"	4.2"	5.4"	5.4"	4.0"

*Could transmit ± 5%, badly aberrated

†The momentum collimator is at 1663" from the B target, which is never exactly at the focus.

≠Mode 4 is as pure at η = 1.5 as mode 3 is at η = 2 because of reduced chromatic aberration.

TABLE II

Gradients and Fields in MESB at 5 GeV/c

In scaling to other momenta, only the bending magnets behave linearly. To scale Q1-Q2-Q3, see Fig. 7. To scale Q4-Q5-Q6, see text. Q7-Q8 scale roughly linearly. For exact information, a computer run is necessary. All bend angles are 8° except D3, which is 3.07° in the West branch and 0° in the East. Positive gradients are focussing horizontally.

agnet	Type	Vert. Gap or Diam.	Eff. Length	Position (B-targ. to center)	Fields (kG) or Gradients (kG/inch)								Max Field
					1W	3W CRAM	3W CMU	3W ROT	4W	1E	3E	4E	
Q1	N8Q32	8"	36"	180"	1.55	0.95	0.95	0.95	0.95	1.55	1.55	0.95	3.3
Q2	N8Q32	8	36	277	- 1.59	+ 0.57	0.54	0.54	0.58	- 1.62	0.57	0.58	3.3
D1	18C72	3.5	75.5	360	12.10	12.10	12.10	12.10	12.10	12.10	12.10	12.10	22.5
Q3	12Q30	12	36	433	0.69	- 0.65	- 0.65	- 0.65	- 0.65	0.75	- 0.65	- 0.65	2.7
Q4	12Q30	12	36	1499	0.84	0.97	1.01	1.07	- 0.89	1.42	1.20	- 1.03	2.7
Q5	8Q24	8	28	1579	- 1.31	- 1.40	- 1.43	- 1.45	+ 1.37	- 1.70	- 1.48	1.79	3.6
S1	12S24	12	26.5	1608	- 0.60*	- 0.12*	0	0	- 0.18*	*	- 0.16*	?	1.25
S2	12S24	12	26.5	1721	0	0	- 0.28*	- 0.34*	0	*	0	?	1.25
D2	18D72	2.5	74	1870	12.34	12.34	12.34	12.34	12.34	12.34	12.34	12.34	25
Q6	8Q24	8	28	1943†	0.91	0.67	0.75	0.58	- 0.06	1.18	1.69	1.82	3.6
D3	18D36	1.25	42	2202	8.34	8.34	8.34	8.34	8.34	0	0	0	20.5
D4	18D72	2.5	74	2446(W) 2472(E)	12.34	12.34	12.34	12.34	12.34	12.34	12.34	12.34	25
Q7	12Q30	12	36		- 0.99	- 1.00	+ 1.45	1.21	- 1.29	- 1.61	- 1.57	- 1.56	2.7
Q8	12Q30	12	36		1.44	1.48	- 1.52	- 1.45	1.51	2.26	2.24	2.23	2.7
Q9	8Q48	8	52		----	----	----	1.55	----	----	----	----	2.5 or 3.6

* The x component of the field of a sextupole is given by $B_x = Ksy$. The "Gradient" listed is $\int Kd\ell$.

† 2093" in mode 3E.

TABLE III. Properties of the MESB at Various Final Foci

The full widths (Δx, Δy) include 95% of the particles, but do not include the large effects of multiple scattering in the beam Cerenkov chambers. The full angles ($\Delta x'$, $\Delta y'$) include 99% of the particles. The transmission is the fraction of the particles in the initial phase space (see TABLE I) which reach the second focus; the average transmission (70%) has been folded into the flux curves (Figs. 8-12). See text for discussion.

	MODE							
	1W	3W CRAM	3W CMU	3W ROT	4W	1E	3E	4E
Distance from B-targ. to:								
Q7 Center	2796"	2796	2796	2645	2796	2645	2645	2645
Q8 Center	2984"	2984	2874	2845	2904	2753	2753	2753
Q9 Center	----	----	----	3015	----	----	----	----
Target Magnification at final focus:								
MV	3.51	0.75	0.25	0.53	1.05	2.66	0.60	1.33
MH	1.20	1.79	4.33	0.53	1.77	0.57	0.53	1.17
Full widths at final focus:								
Δx	0.45"	0.38	1.6	0.40	0.40	0.45	0.40	0.40
$\Delta x'$	52 mr	60	15	11	44	64	80	52
Δy	0.25"	0.19	0.20	1.3	0.10	0.20	0.20	0.20
$\Delta y'$	4.4 mr	4.0	9.0	22	2.4	5.6	5.6	3.2
$\Delta x \Delta x'$	23 mr"	23	24	4.4	17	29	32	21
$\Delta y \Delta y'$	1.10 mr"	0.76	1.8	29	0.24	1.1	1.1	0.64
Transmission	77%	72	75	70	74	65	61	77
% which scrape Q8	3%	3	0	5	7	0	20	0

TABLE IV. Approximate Beam Sizes at Various Places Along the Beam

The quantity listed is (Δx) x (Δy), where Δx = horizontal full width, Δy = vertical full width, in inches. These widths include 100% of the particles (or more, in the case of Δy where the histogram bin size is sometimes too big). The widths are based on ray plots up to PLIM and on Monte Carlo's thereafter. In the MPS modes, sizes beyond the mass slit depend upon the final focussing method as shown. "CRAM" is the small horizontal spot size with large divergence. "CMU" is the big horizontal spot size with small divergence. "ROT" is phase space interchange with a rotated triplet. Full momentum bite and a 4" B-target are assumed. MPS1 is blank frequently since it has not been studied past MASS.

MODE / Position	E1	E3	MPS1			MPS3			MPS4
			CRAM	CMU	ROT	CRAM	CMU	ROT	CRAM
Q3 end	10.6x2.0	6.0x2.0	11.0 x 2.0			4.8 x 2.0			4.8x2.0
Q4 end	12.0x3.2	12.0x2.6	11.0 x 3.0			12.0 x 2.0			8.5x2.0
PLIM*	1.8x3.0	4.4x2.6	5.3x3.3			6.3x2.5	6.0x2.5	5.5x2.5	7.4x1.1
Q6 end	8.4x0.8	6.0x0.4	8.4x0.8			8.4x0.8	7.8x0.8	6.0x1.2	4.8x0.8
Mass Slit†	5.4x1.3	5.4x0.3	6.0x1.3			6.0x0.3	5.4x0.3	5.4x0.3	4.2x
D3 end	4.2x0.8	3.6x0.6	6.0x0.4			5.4x0.4	4.2x0.4	5.4x0.4	4.2x0.4
D4 end	3.6x1.6	5.4x1.8	5.4x1.6			5.4x1.6	6.0x1.6	7.2x1.2	6.0x1.2
Q7 begin	5.6x2.0	8.8x2.4	8.0x2.4			8.0x2.6	10.4x2.6	8.0x1.6	9.6x1.6
Q8 begin	10.4x1.0	18.0x1.2ϟ	16.0x1.2ϟ			16.0x1.2ϟ	6.4x4.2	11.2x11.2	16.0x1.0ϟ
Q8 + 44"	6.5x0.4	8.4x0.8	9.0x0.8		---	9.0x0.8	4.5x4.0	-----	10.8x0.8
Q9 begin	-----	-----	-----	---		-----	-----	2.5x6.0	-----
Q9 + 44"	-----	-----	-----	---		-----	-----	2.0x4.0	-----
MPS-targ.	-----	-----	0.6x0.5			0.5x0.2	2.2x2.6+	0.4x1.1	0.5x0.2
East-targ.	.60x.65	0.75x0.35	-----	---	---	-----	-----	-----	-----

* Momentum collimator, assumed to be set at the center of image of off-momentum particles at full bite.

† In vertical plane, includes π's, K's and $\bar{p}$'s, at momentum where $\eta = 2$.

ϟ Scrapes.

\+ LH2 target in front of MPS magnet.

Figure Captions

Fig. 1 Beam Layout

Fig. 2 Optics of Mode 1E

Fig. 3 Optics of Mode 3E

Fig. 4 Optics of Mode 1W

Fig. 5 Optics of Mode 3W CRAM

Fig. 6 Optics of Mode 4W

Fig. 7 Gradients of quadrupoles Q1, Q2, Q3 vs. momentum at which $\eta = 2$, for K separation and $\bar{p}$ separation.

Figs. 8 - 10 Fluxes of particles at the two final foci per 10^{12} interacting protons in a beryllium target, assuming Sanford + Wang. The curves assume the full solid angle and momentum bites of Table I and a 70% transmission through the beam. For genuine numbers of particles at the end of beam, multiply by the number of protons in the external beam and the fractions which interact in the target.

Fig. 11 $\pi^-:K^-$ and $\pi^-:\bar{p}$ ratio in front of mass slit as a function of momentum.

Fig. 12 Variation of $\int Bd\ell$ as a function of horizontal position in D1.

Fig. 13 $\int Bd\ell$ as a function of current for D1. The measured values extend to 3.0 kA. Taking $\int Bd\ell/I = 500$ kG in /kA at 3.4 kA gives $P_{max} = 9.24 \pm .2$ GeV/c. For 510 kG in /kA, $P_{max} = 9.43$ GeV/c.

Fig. 14 Expected momentum distributions for several modes. The momentum collimator was set at the centers of the images of particles with $\Delta p/p = \pm 3\%$ and $\pm 2\text{-}1/2\%$ for modes 1 and 3, respectively.

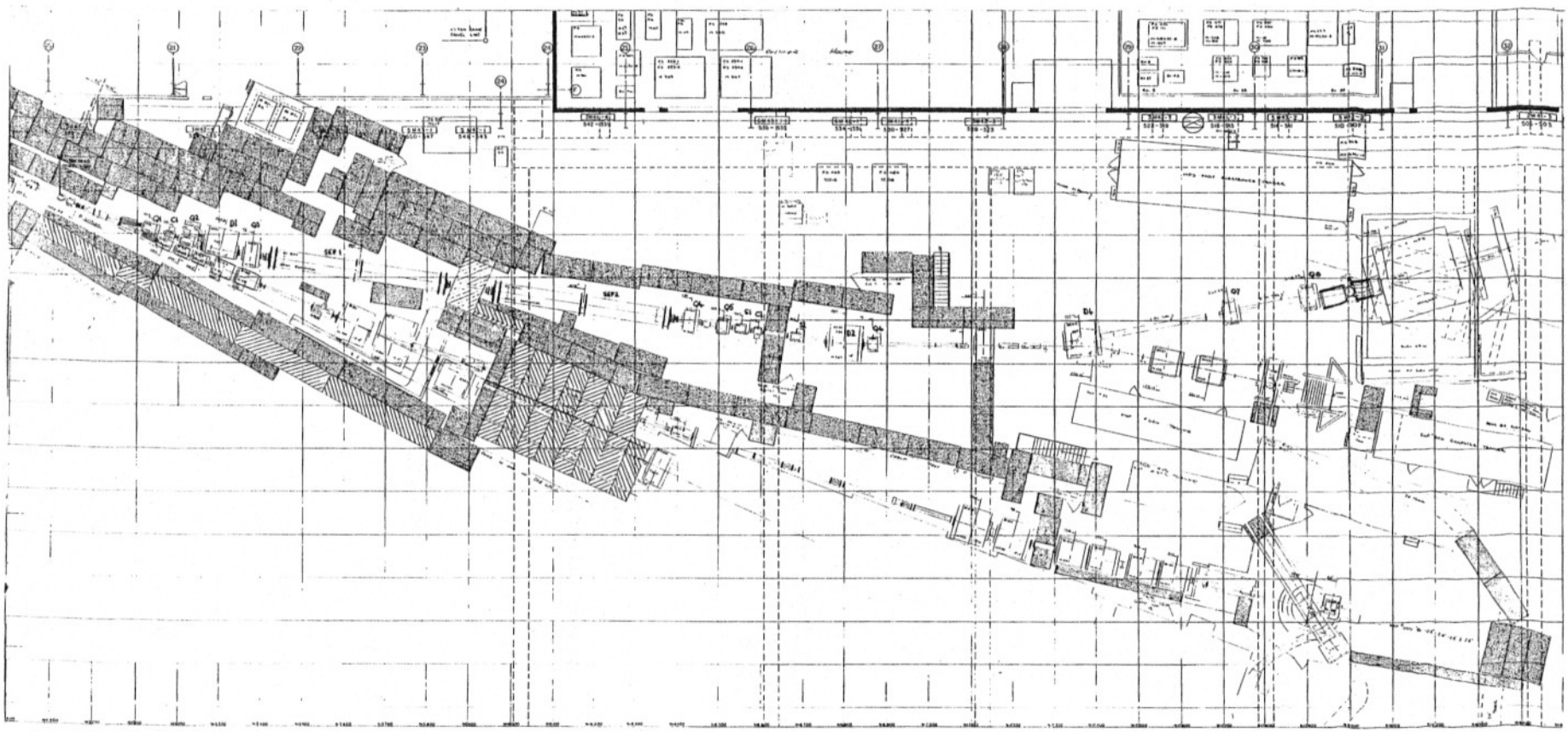

Figure 1

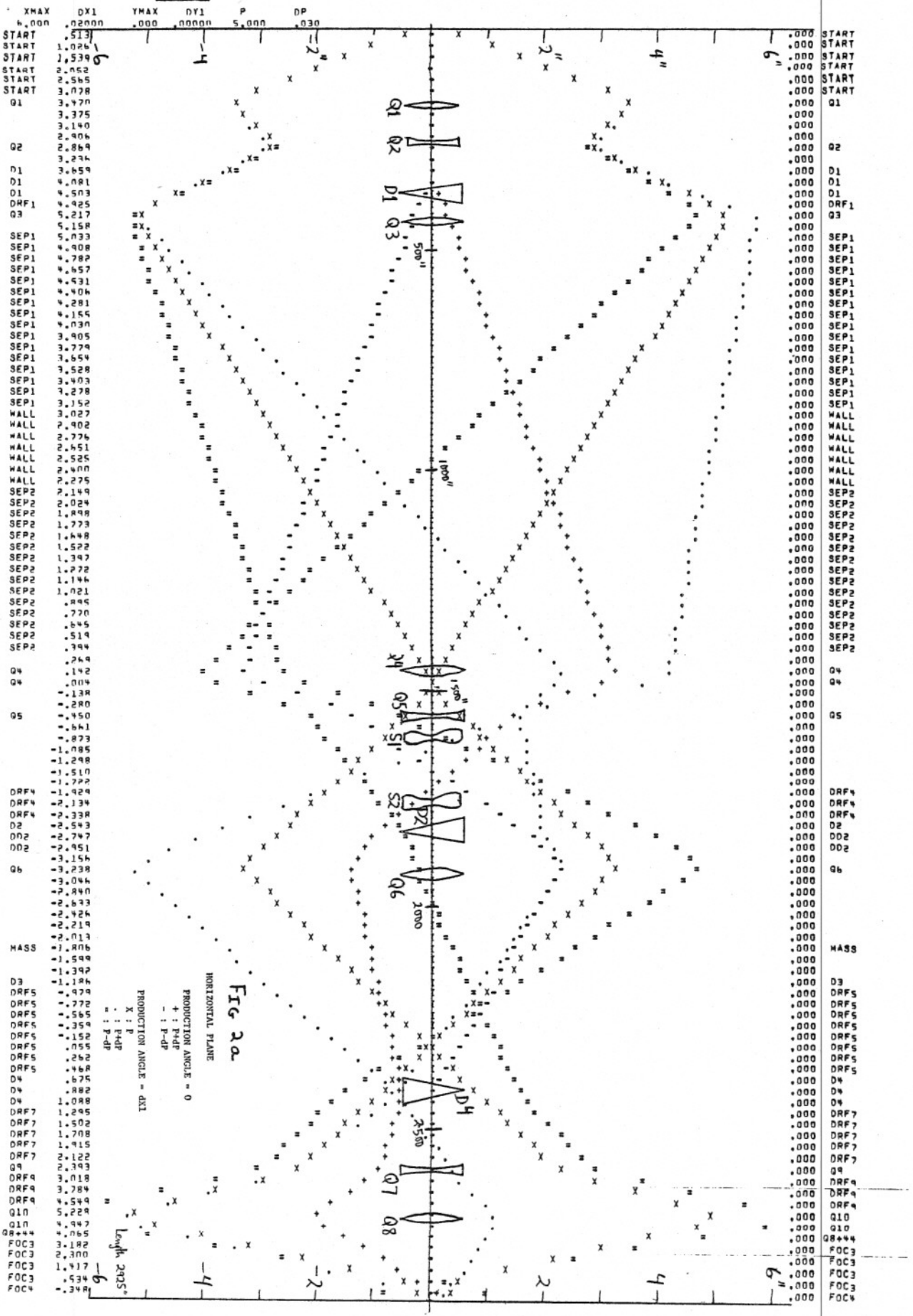
XMAX DX1 YMAX DY1 P DP
4.000 .02000 .000 .00000 5.000 .030
Q1
Q2
D1
Q3
Q4
Q5
S1
S2
D2
Q6
D4
Q7
Q8
500"
1000"
1500"
2000
2500
Length 2925"
HORIZONTAL PLANE
PRODUCTION ANGLE = 0
+ : P+dP
- : P-dP
PRODUCTION ANGLE = dX1
X : P
= : P+dP
: P-dP

Fig 2a

XMAX	DX1	YMAX	DY1	P	DP
-6.000	.02000	3.000	.00320	5.000	.030

Fig 2b

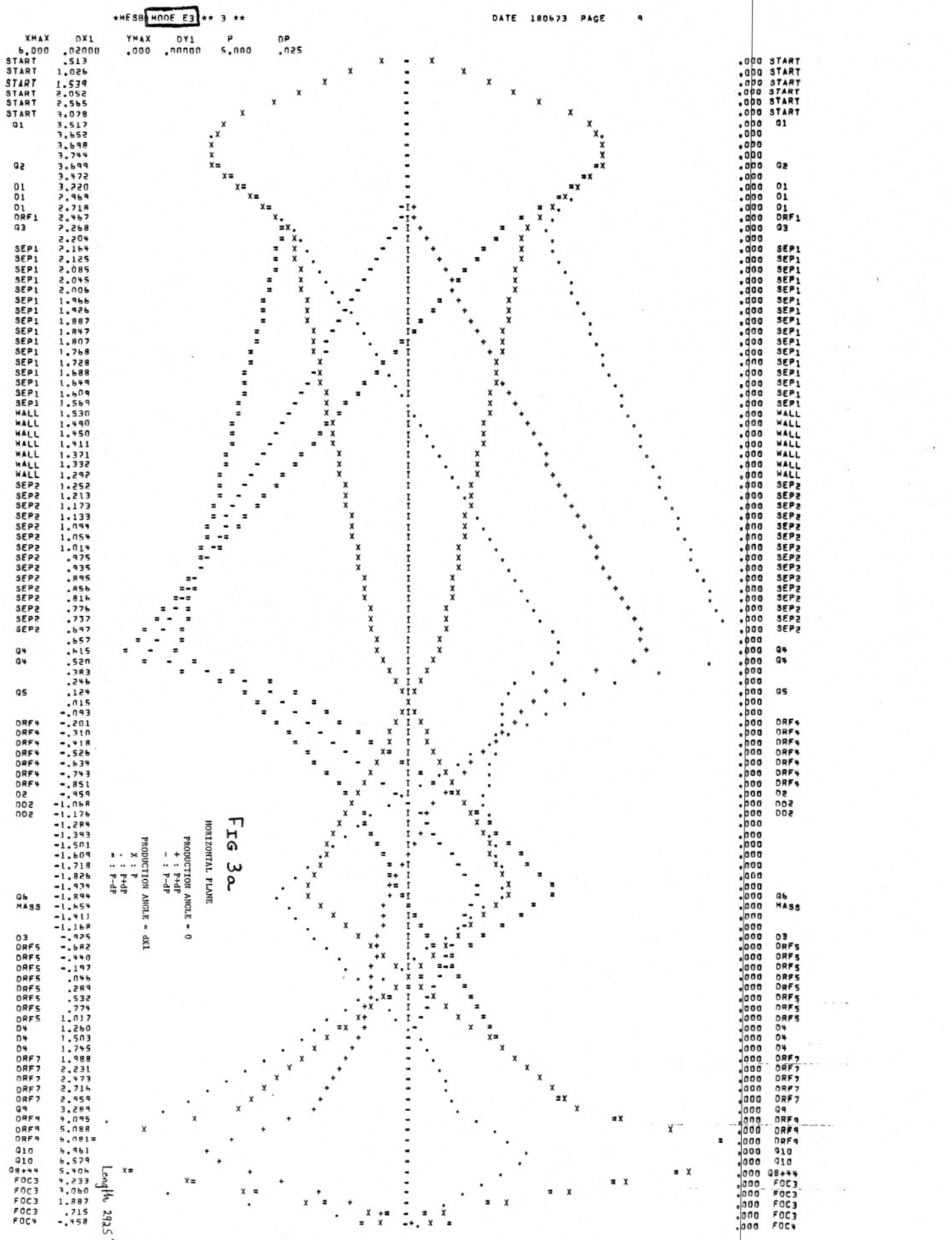
*MESH MODE E3 ** 3 **
DATE 180673 PAGE 9
XMAX DX1 YMAX DY1 P DP
6.000 .02000 .000 .00000 5.000 .025
PRODUCTION ANGLE = dX1
X : P
- : P+dP
= : P-dP
PRODUCTION ANGLE = 0
+ : P+dP
- : P-dP
HORIZONTAL PLANE
Length 29.5"

Fig 3a

XMAX	DX1	YMAX	DY1	P	DP
-6.000	.02000	3.000	.00115	5.000	.025

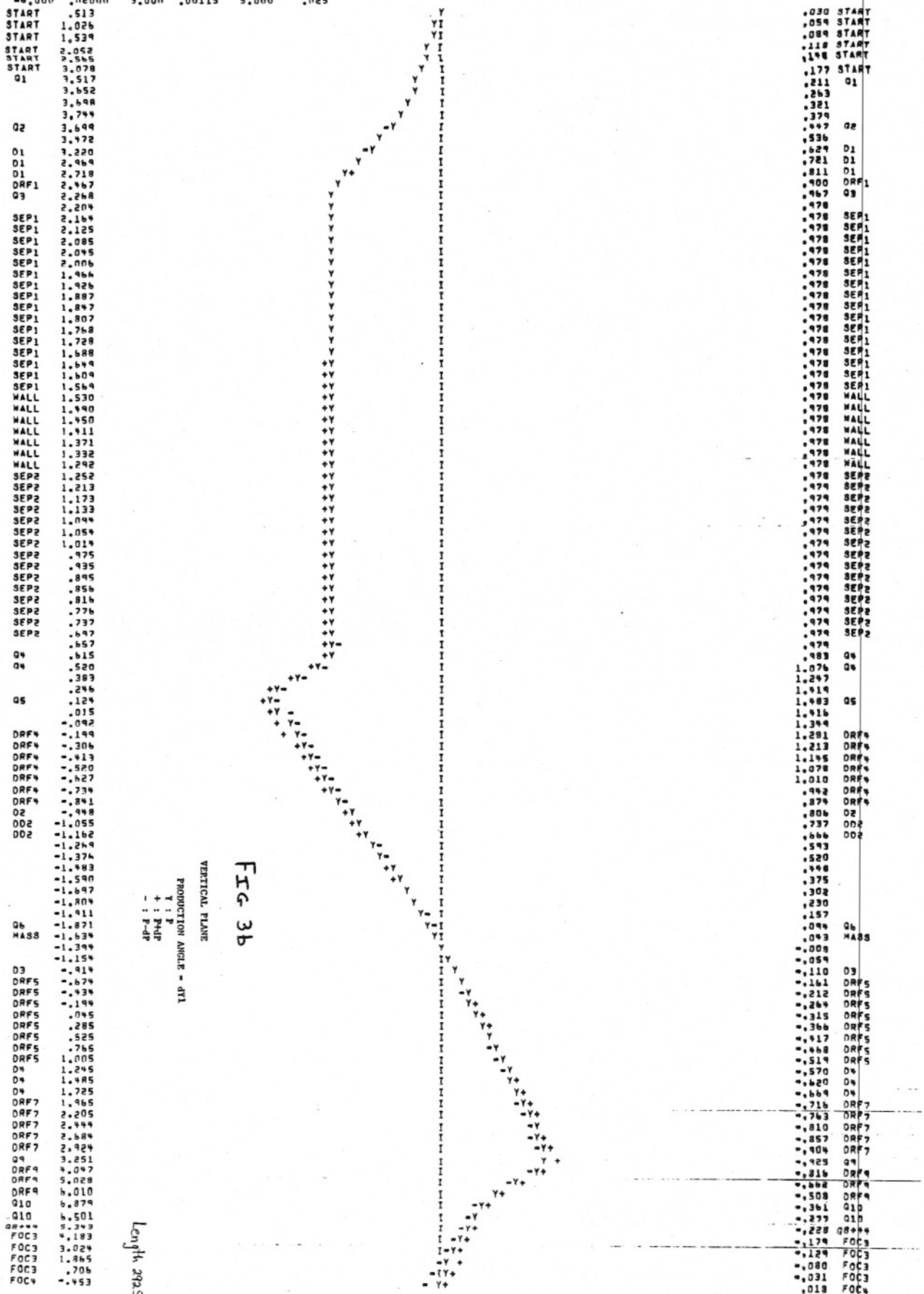

Fig 3b

Length 2925"

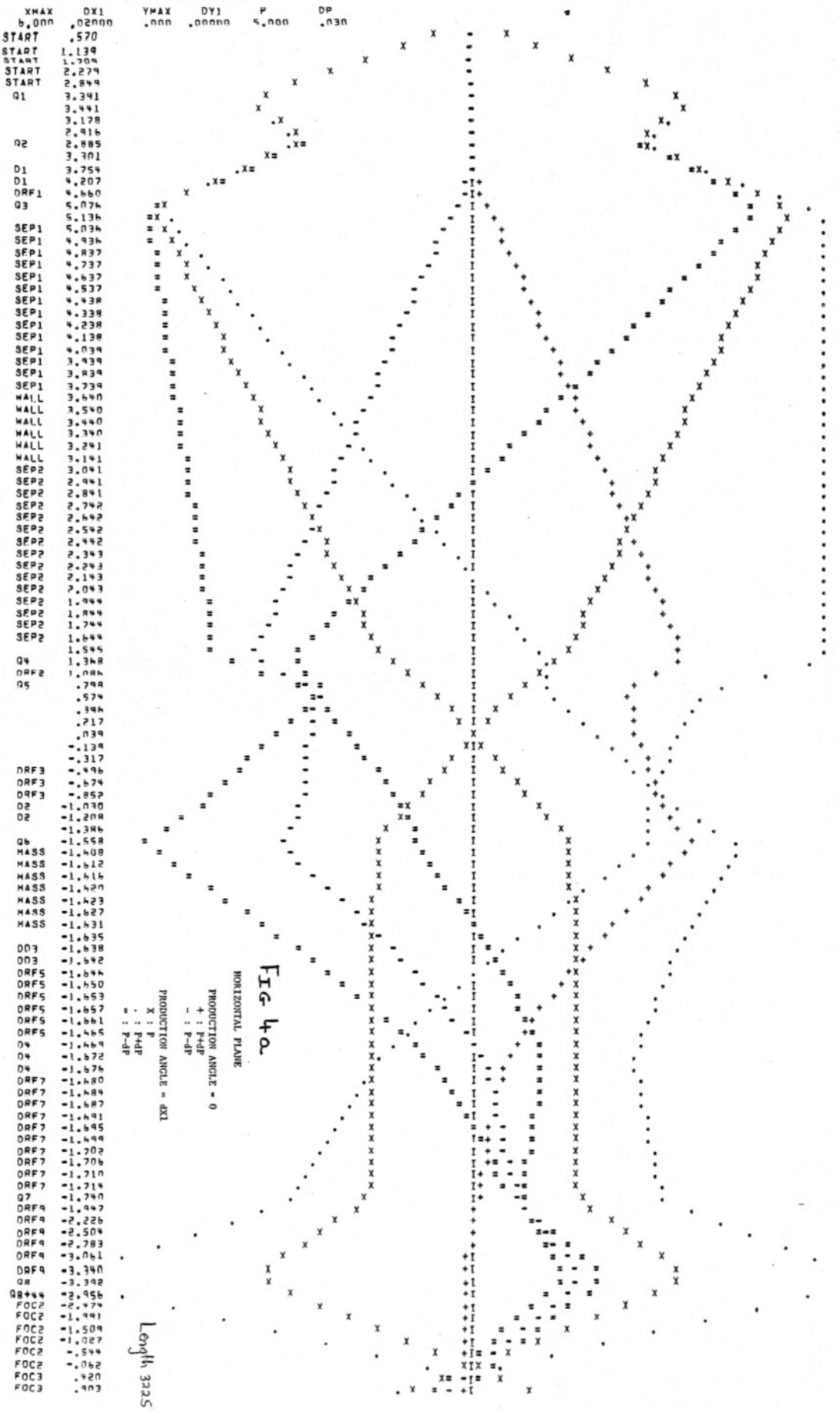
XMAX DX1 YMAX DY1 P DP
6.000 .02000 .000 .00000 5.000 .030
START .570
START 1.139
START 1.709
START 2.279
START 2.849
Q1 3.391
3.441
3.178
2.916
Q2 2.885
3.301
D1 3.754
D1 4.207
DRF1 4.660
Q3 5.074
5.134
SEP1 5.034
SEP1 4.934
SEP1 4.837
SEP1 4.737
SEP1 4.637
SEP1 4.537
SEP1 4.438
SEP1 4.338
SEP1 4.238
SEP1 4.138
SEP1 4.039
SEP1 3.939
SEP1 3.839
SEP1 3.739
WALL 3.640
WALL 3.540
WALL 3.440
WALL 3.340
WALL 3.241
WALL 3.141
SEP2 3.041
SEP2 2.941
SEP2 2.841
SEP2 2.742
SEP2 2.642
SEP2 2.542
SEP2 2.442
SEP2 2.343
SEP2 2.243
SEP2 2.143
SEP2 2.043
SEP2 1.944
SEP2 1.844
SEP2 1.744
SEP2 1.644
1.545
Q4 1.348
DRF2 1.086
Q5 .798
.574
.394
.217
.039
-.139
-.317
DRF3 -.496
DRF3 -.674
DRF3 -.852
D2 -1.030
D2 -1.208
-1.386
Q6 -1.558
MASS -1.608
MASS -1.612
MASS -1.616
MASS -1.620
MASS -1.623
MASS -1.627
MASS -1.631
-1.635
DD3 -1.638
DD3 -1.642
DRF5 -1.644
DRF5 -1.650
DRF5 -1.653
DRF5 -1.657
DRF5 -1.661
DRF5 -1.665
D4 -1.669
D4 -1.672
D4 -1.676
DRF7 -1.680
DRF7 -1.684
DRF7 -1.687
DRF7 -1.691
DRF7 -1.695
DRF7 -1.699
DRF7 -1.702
DRF7 -1.706
DRF7 -1.710
DRF7 -1.714
Q7 -1.740
DRF9 -1.947
DRF9 -2.226
DRF9 -2.504
DRF9 -2.783
DRF9 -3.061
DRF9 -3.340
Q8 -3.398
Q8+++ -2.956
FOC2 -2.479
FOC2 -1.991
FOC2 -1.509
FOC2 -1.027
FOC2 -.544
FOC2 -.062
FOC3 .420
FOC3 .903
PRODUCTION ANGLE = dX1
X : P
. : P+dP
= : P-dP
PRODUCTION ANGLE = 0
+ : P+dP
- : P-dP
HORIZONTAL PLANE
Length 3225"
.000 START
.000 START
.000 START
.000 START
.000 START
.000 Q1
.000
.000
.000
.000 Q2
.000
.000 D1
.000 D1
.000 DRF1
.000 Q3
.000
.000 SEP1
.000 SEP1
.000 SEP1
.000 SEP1
.000 SEP1
.000 SEP1
.000 SEP1
.000 SEP1
.000 SEP1
.000 SEP1
.000 SEP1
.000 SEP1
.000 SEP1
.000 SEP1
.000 WALL
.000 WALL
.000 WALL
.000 WALL
.000 WALL
.000 WALL
.000 SEP2
.000 SEP2
.000 SEP2
.000 SEP2
.000 SEP2
.000 SEP2
.000 SEP2
.000 SEP2
.000 SEP2
.000 SEP2
.000 SEP2
.000 SEP2
.000 SEP2
.000 SEP2
.000
.000 Q4
.000 DRF2
.000 Q5
.000
.000
.000
.000
.000
.000
.000 DRF3
.000 DRF3
.000 DRF3
.000 D2
.000 D2
.000
.000 Q6
.000 MASS
.000 MASS
.000 MASS
.000 MASS
.000 MASS
.000 MASS
.000 MASS
.000
.000 DD3
.000 DD3
.000 DRF5
.000 DRF5
.000 DRF5
.000 DRF5
.000 DRF5
.000 DRF5
.000 D4
.000 D4
.000 D4
.000 DRF7
.000 DRF7
.000 DRF7
.000 DRF7
.000 DRF7
.000 DRF7
.000 DRF7
.000 DRF7
.000 DRF7
.000 DRF7
.000 Q7
.000 DRF9
.000 DRF9
.000 DRF9
.000 DRF9
.000 DRF9
.000 DRF9
.000 Q8
.000 Q8+++
.000 FOC2
.000 FOC2
.000 FOC2
.000 FOC2
.000 FOC2
.000 FOC2
.000 FOC3
.000 FOC3

FIG 4a

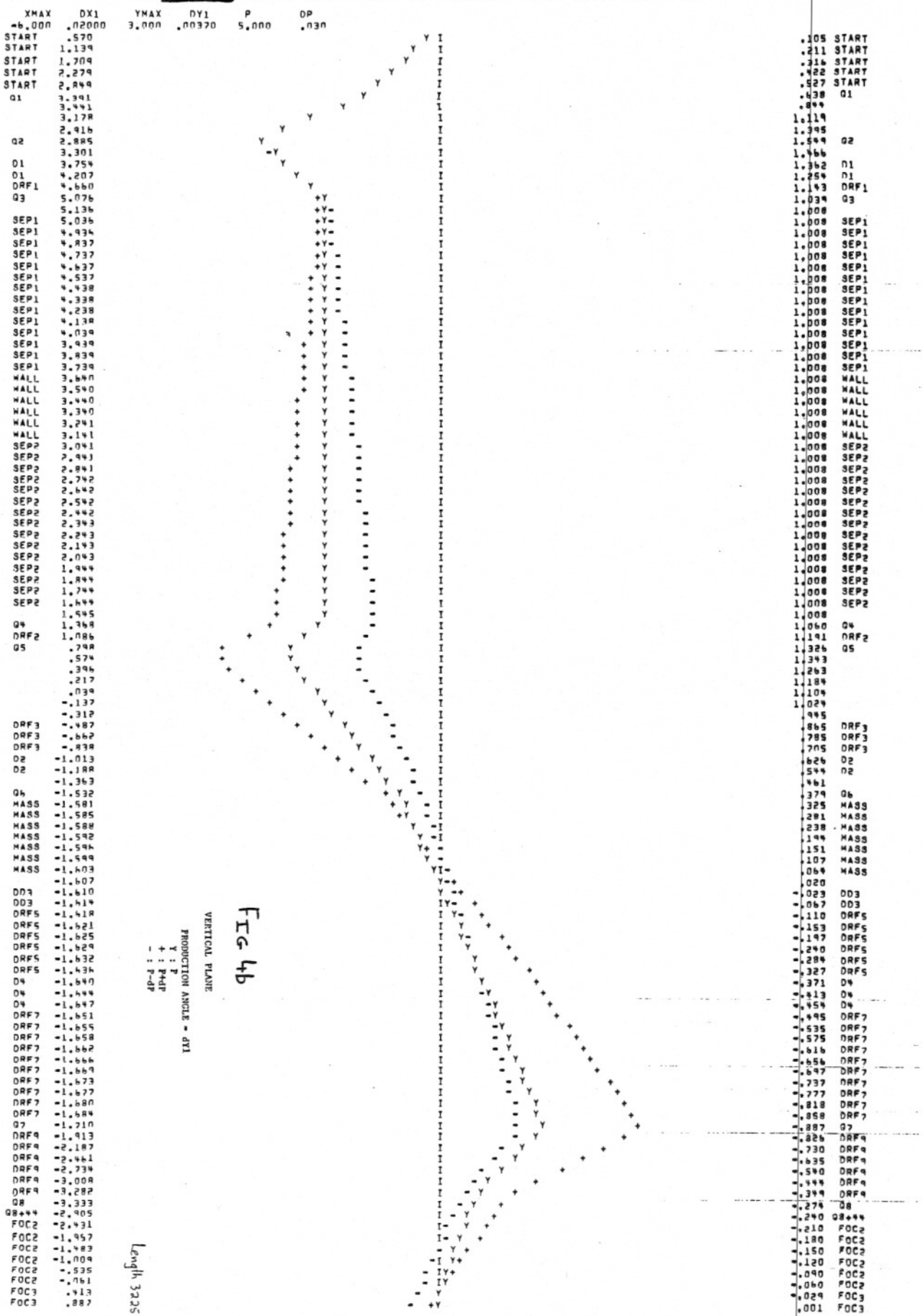

Fig 4b

Length 325"

MESB, MODE MPS 3 ** 3 ** CRAM IT AL IN 12 INCH TARGET DATE 180673 PAGE 9

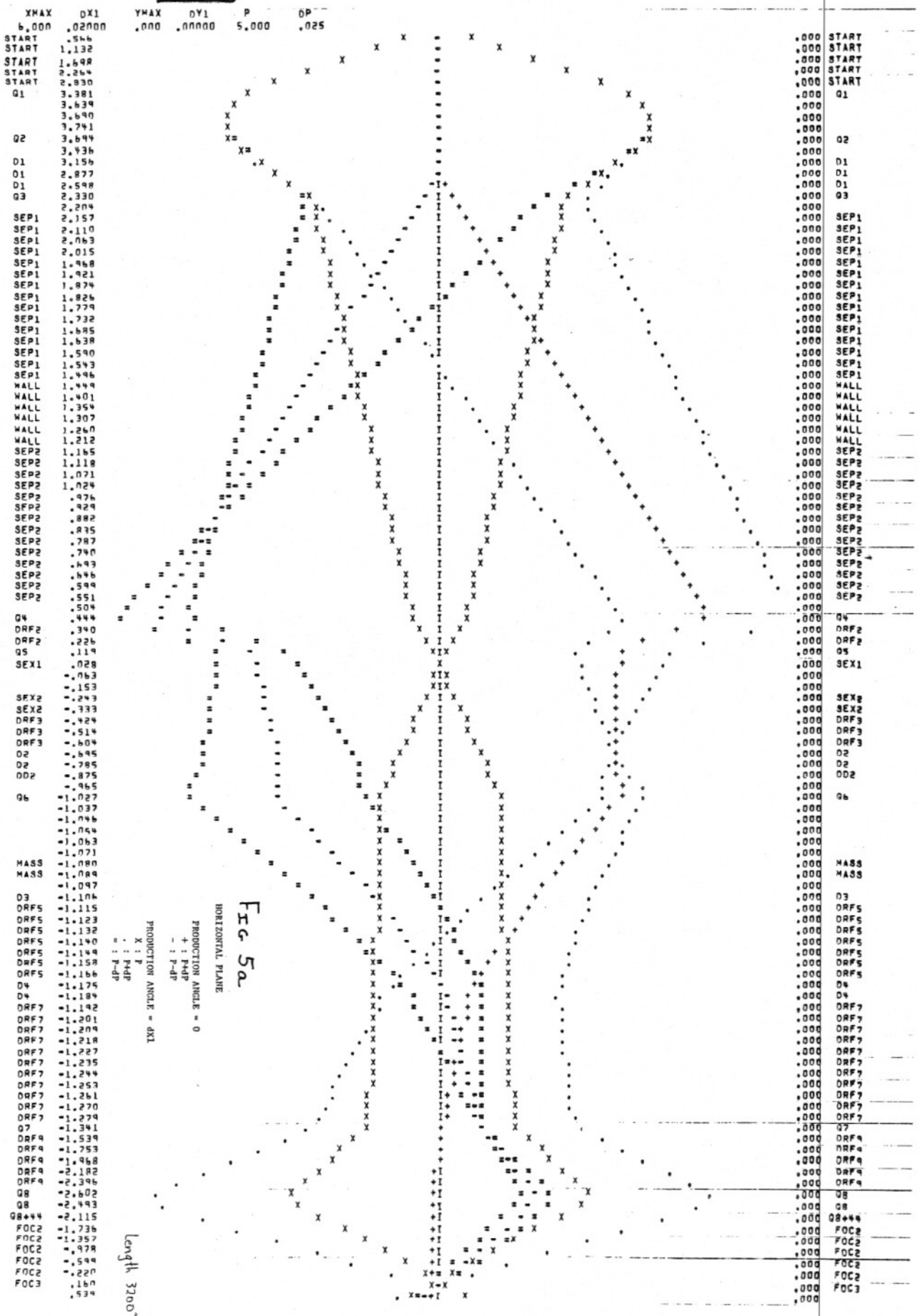

Fig 5a

Length 3200"

XMAX	DX1	YMAX	DY1	P	DP
-6.000	.02000	3.000	.00115	5.000	.025

START	.566	.033	START
START	1.132	.065	START
START	1.698	.098	START
START	2.264	.130	START
START	2.830	.163	START
Q1	3.381	.196	Q1
	3.639	.247	
	3.690	.311	
	3.741	.375	
Q2	3.694	.449	Q2
	3.436	.549	
D1	3.156	.651	D1
D1	2.877	.752	D1
D1	2.598	.851	D1
Q3	2.330	.944	Q3
	2.204	.978	
SEP1	2.157	.978	SEP1
SEP1	2.110	.978	SEP1
SEP1	2.063	.978	SEP1
SEP1	2.015	.978	SEP1
SEP1	1.968	.978	SEP1
SEP1	1.921	.979	SEP1
SEP1	1.874	.979	SEP1
SEP1	1.826	.979	SEP1
SEP1	1.779	.979	SEP1
SEP1	1.732	.979	SEP1
SEP1	1.685	.979	SEP1
SEP1	1.638	.979	SEP1
SEP1	1.590	.979	SEP1
SEP1	1.543	.979	SEP1
SEP1	1.496	.979	SEP1
WALL	1.449	.979	WALL
WALL	1.401	.979	WALL
WALL	1.354	.979	WALL
WALL	1.307	.979	WALL
WALL	1.260	.979	WALL
WALL	1.212	.979	WALL
SEP2	1.165	.979	SEP2
SEP2	1.118	.979	SEP2
SEP2	1.071	.979	SEP2
SEP2	1.024	.979	SEP2
SEP2	.976	.979	SEP2
SEP2	.929	.979	SEP2
SEP2	.882	.979	SEP2
SEP2	.835	.979	SEP2
SEP2	.787	.979	SEP2
SEP2	.740	.979	SEP2
SEP2	.693	.979	SEP2
SEP2	.646	.979	SEP2
SEP2	.599	.979	SEP2
SEP2	.551	.980	SEP2
	.504	.980	
Q4	.444	1.005	Q4
DRF2	.340	1.134	DRF2
DRF2	.226	1.286	DRF2
Q5	.119	1.382	Q5
SEX1	.028	1.313	SEX1
	-.062	1.234	
	-.151	1.156	
SEX2	-.241	1.077	SEX2
SEX2	-.330	.998	SEX2
DRF3	-.420	.919	DRF3
DRF3	-.509	.840	DRF3
DRF3	-.598	.762	DRF3
D2	-.688	.683	D2
D2	-.777	.603	D2
DD2	-.867	.521	DD2
	-.956	.438	
Q6	-1.017	.366	Q6
	-1.027	.314	
	-1.035	.262	
	-1.044	.211	
	-1.053	.159	
	-1.061	.107	
MASS	-1.070	.055	MASS
MASS	-1.078	.003	MASS
	-1.087	-.048	
D3	-1.095	-.100	D3
DRF5	-1.104	-.152	DRF5
DRF5	-1.112	-.203	DRF5
DRF5	-1.121	-.255	DRF5
DRF5	-1.129	-.307	DRF5
DRF5	-1.138	-.358	DRF5
DRF5	-1.147	-.410	DRF5
DRF5	-1.155	-.461	DRF5
D4	-1.164	-.513	D4
D4	-1.172	-.562	D4
DRF7	-1.181	-.610	DRF7
DRF7	-1.189	-.658	DRF7
DRF7	-1.198	-.706	DRF7
DRF7	-1.206	-.753	DRF7
DRF7	-1.215	-.801	DRF7
DRF7	-1.223	-.849	DRF7
DRF7	-1.232	-.896	DRF7
DRF7	-1.240	-.944	DRF7
DRF7	-1.249	-.992	DRF7
DRF7	-1.258	-1.039	DRF7
DRF7	-1.266	-1.087	DRF7
Q7	-1.328	-1.088	Q7
DRF9	-1.524	-.980	DRF9
DRF9	-1.736	-.859	DRF9
DRF9	-1.949	-.738	DRF9
DRF9	-2.161	-.617	DRF9
DRF9	-2.373	-.496	DRF9
Q8	-2.577	-.376	Q8
Q8	-2.469	-.300	Q8
Q8+44	-2.095	-.257	Q8+44
FOC2	-1.719	-.214	FOC2
FOC2	-1.344	-.170	FOC2
FOC2	-.968	-.127	FOC2
FOC2	-.593	-.084	FOC2
FOC2	-.217	-.041	FOC2
FOC3	.158	.002	FOC3
	.533	.045	

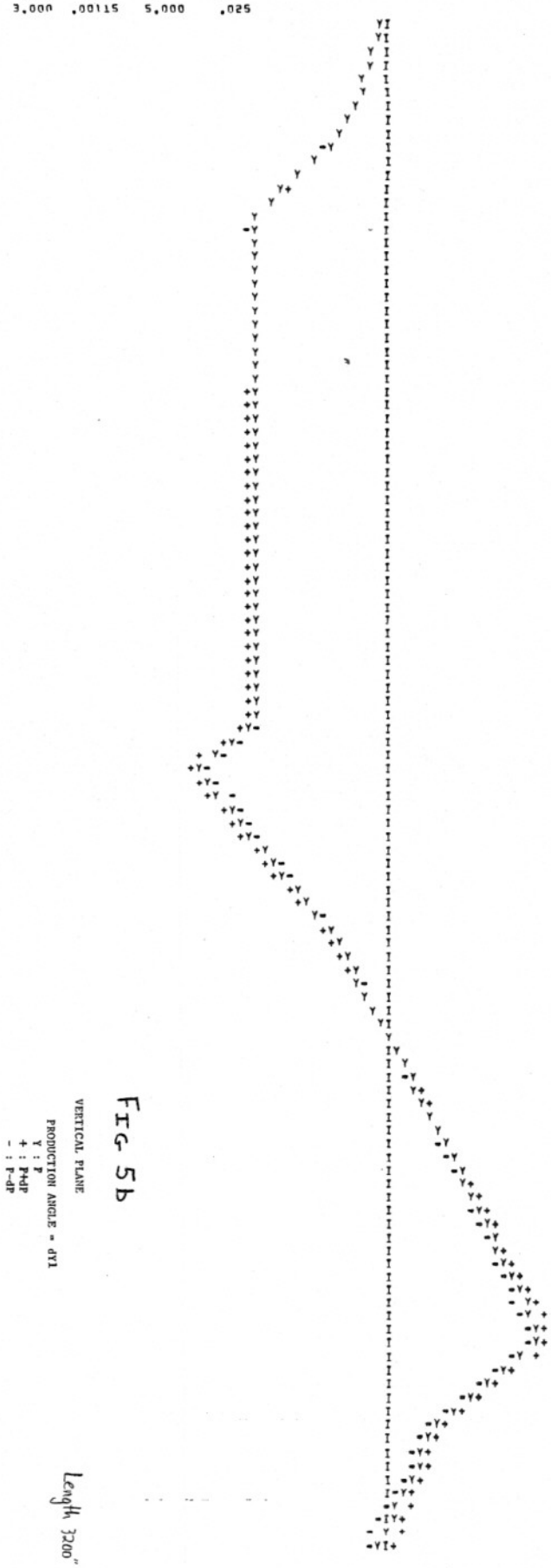

VERTICAL PLANE

PRODUCTION ANGLE = dY1

Y : P

+ : P+dP

- : P-dP

FIG 5b

Length 3200"

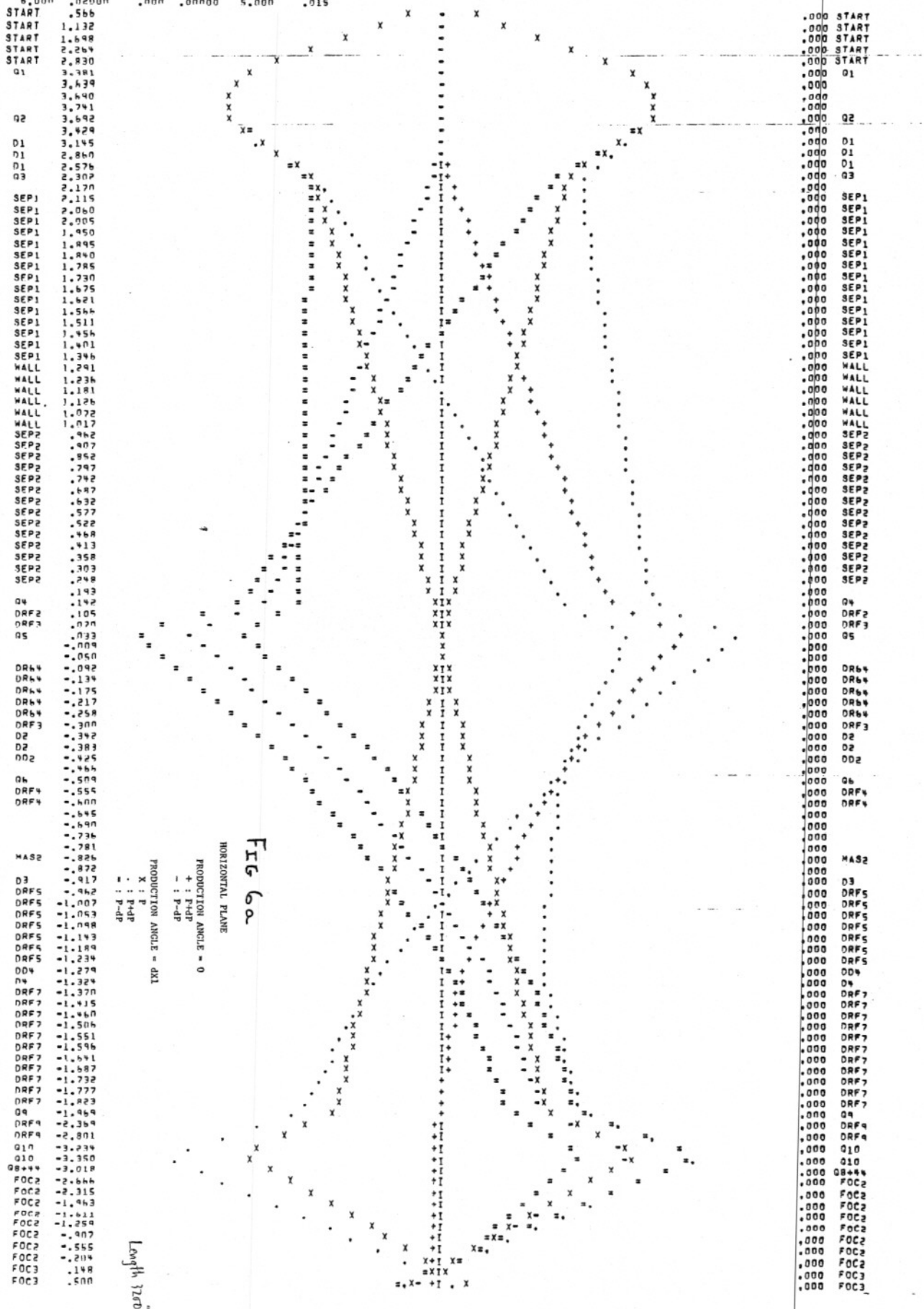
B E A M MPS 4 * 4 **
DATE 180673 PAGE 9
XMAX DX1 YMAX DY1 P DP
6.000 .02000 .000 .00000 5.000 .015
START .566
START 1.132
START 1.698
START 2.264
START 2.830
Q1 3.381
3.639
3.690
3.741
Q2 3.692
3.429
D1 3.145
D1 2.860
D1 2.576
Q3 2.302
2.170
SEP1 2.115
SEP1 2.060
SEP1 2.005
SEP1 1.950
SEP1 1.895
SEP1 1.840
SEP1 1.785
SEP1 1.730
SEP1 1.675
SEP1 1.621
SEP1 1.566
SEP1 1.511
SEP1 1.456
SEP1 1.401
SEP1 1.346
WALL 1.291
WALL 1.236
WALL 1.181
WALL 1.126
WALL 1.072
WALL 1.017
SEP2 .962
SEP2 .907
SEP2 .852
SEP2 .797
SEP2 .742
SEP2 .687
SEP2 .632
SEP2 .577
SEP2 .522
SEP2 .468
SEP2 .413
SEP2 .358
SEP2 .303
SEP2 .248
.193
Q4 .142
DRF2 .105
DRF3 .070
Q5 .033
-.009
-.050
DR64 -.092
DR64 -.134
DR64 -.175
DR64 -.217
DR64 -.258
DRF3 -.300
D2 -.342
D2 -.383
DD2 -.425
-.466
Q6 -.509
DRF4 -.555
DRF4 -.600
-.645
-.690
-.736
-.781
MAS2 -.826
-.872
D3 -.917
DRF5 -.962
DRF5 -1.007
DRF5 -1.053
DRF5 -1.098
DRF5 -1.143
DRF5 -1.189
DRF5 -1.234
DD4 -1.279
D4 -1.324
DRF7 -1.370
DRF7 -1.415
DRF7 -1.460
DRF7 -1.506
DRF7 -1.551
DRF7 -1.596
DRF7 -1.641
DRF7 -1.687
DRF7 -1.732
DRF7 -1.777
DRF7 -1.823
Q9 -1.969
DRF9 -2.369
DRF9 -2.801
Q10 -3.234
Q10 -3.350
Q8+44 -3.018
FOC2 -2.666
FOC2 -2.315
FOC2 -1.963
FOC2 -1.611
FOC2 -1.259
FOC2 -.907
FOC2 -.555
FOC2 -.204
FOC3 .148
FOC3 .500
.000 START
.000 Q1
.000 Q2
.000 D1
.000 D1
.000 D1
.000 Q3
.000 SEP1
.000 WALL
.000 SEP2
.000 Q4
.000 DRF2
.000 DRF3
.000 Q5
.000 DR64
.000 DRF3
.000 D2
.000 DD2
.000 Q6
.000 DRF4
.000 MAS2
.000 D3
.000 DRF5
.000 DD4
.000 D4
.000 DRF7
.000 Q9
.000 DRF9
.000 Q10
.000 Q8+44
.000 FOC2
.000 FOC3
HORIZONTAL PLANE
PRODUCTION ANGLE = 0
+ : P+dP
- : P-dP
PRODUCTION ANGLE = dX1
X : P
. : P+dP
= : P-dP
Length 3200"

FIG 6a

XMAX	DX1	YMAX	DY1	P	DP
=6.000	.02000	3.000	.00115	5.000	.015

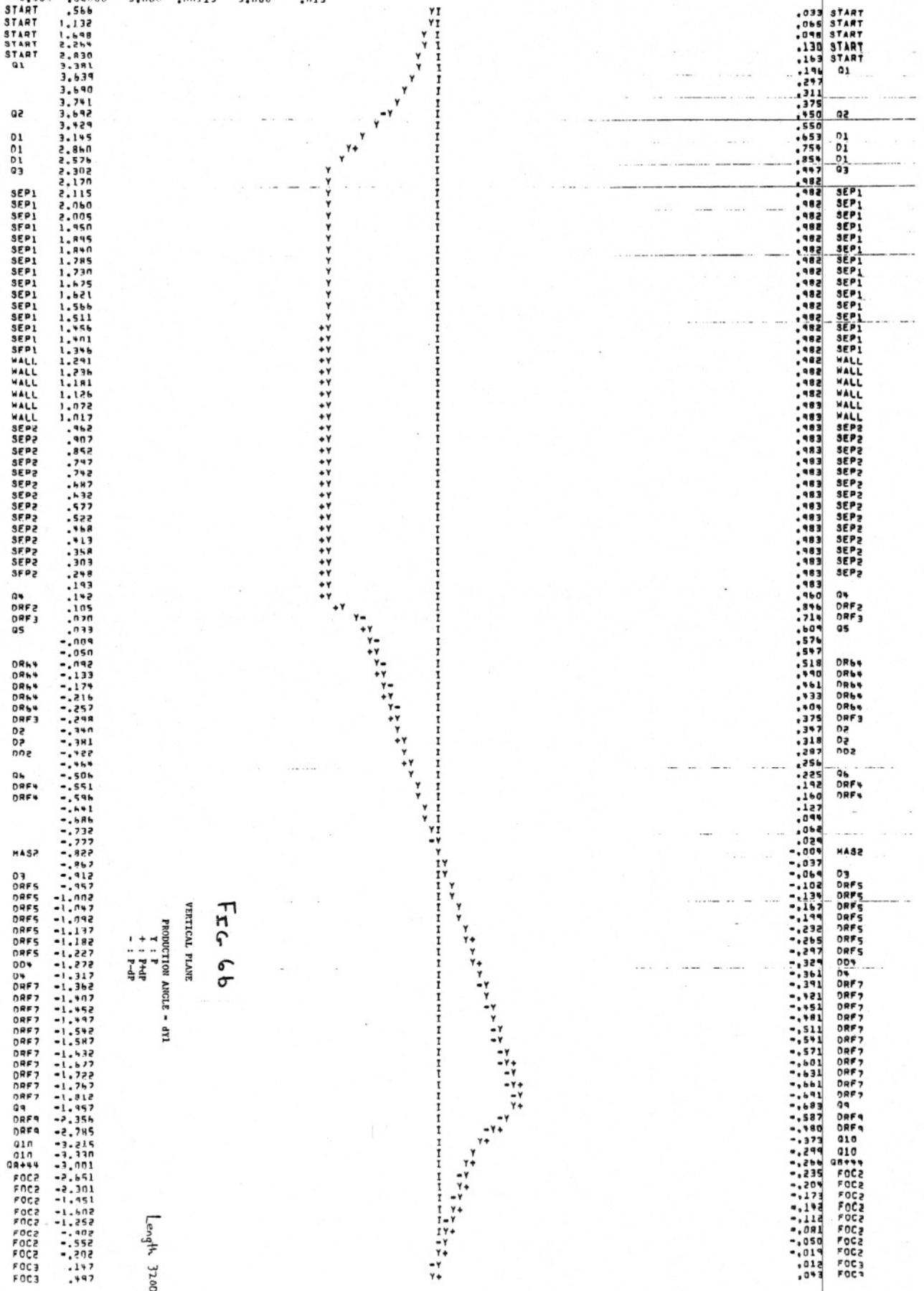

Fig 6b

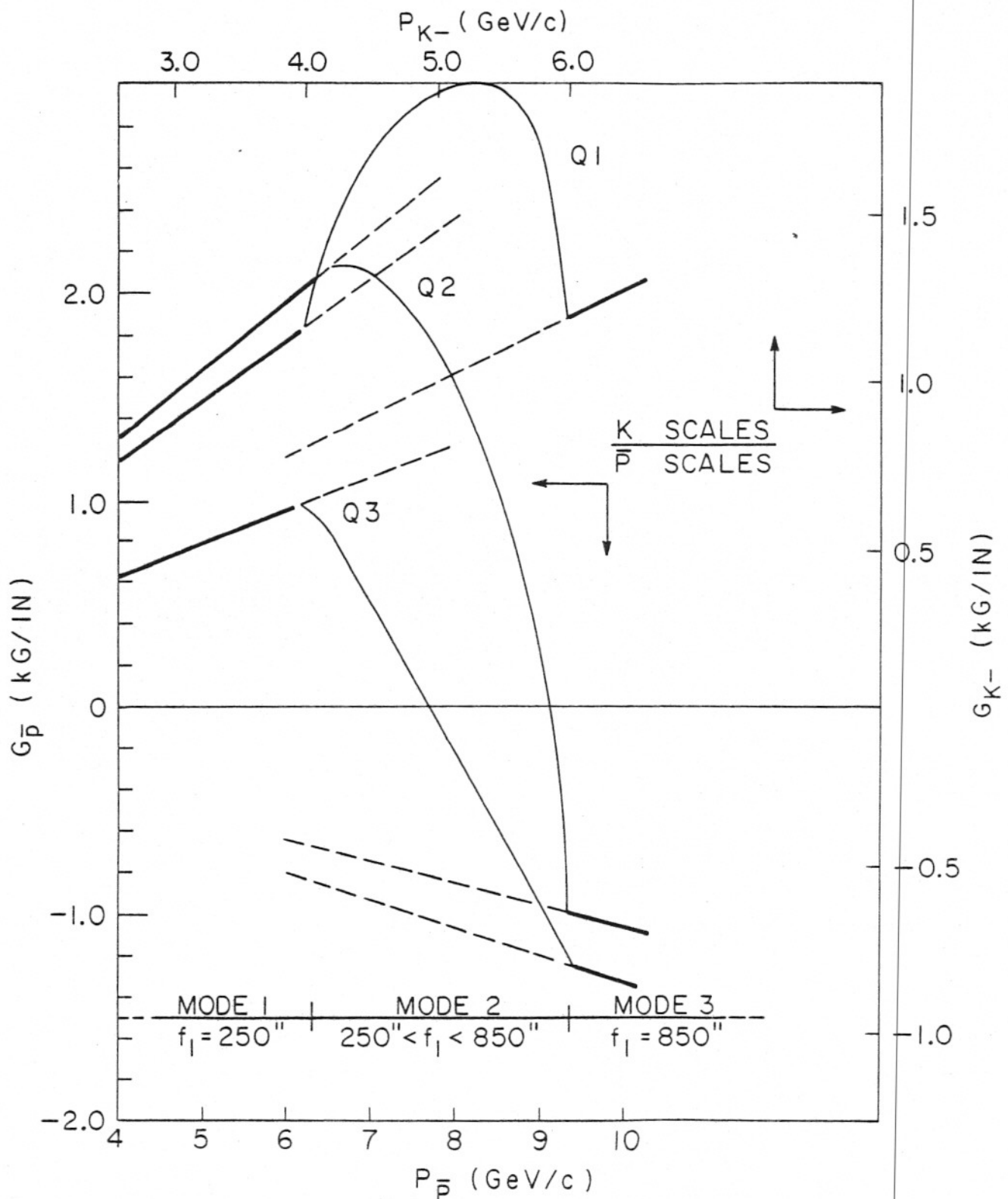
P_{K-} (GeV/c)
3.0
4.0
5.0
6.0
Q1
Q2
Q3
K SCALES
$\bar{P}$ SCALES
MODE 1
$f_1 = 250''$
MODE 2
$250'' < f_1 < 850''$
MODE 3
$f_1 = 850''$
$G_{\bar{p}}$ (kG/IN)
G_{K-} (kG/IN)
2.0
1.0
0
-1.0
-2.0
1.5
1.0
0.5
0.5
1.0
4
5
6
7
8
9
10
$P_{\bar{P}}$ (GeV/c)

Figure 7

XMAX	DX1	YMAX	DY1	P	DP
-6.000	.02000	3.000	.00115	5.000	.015

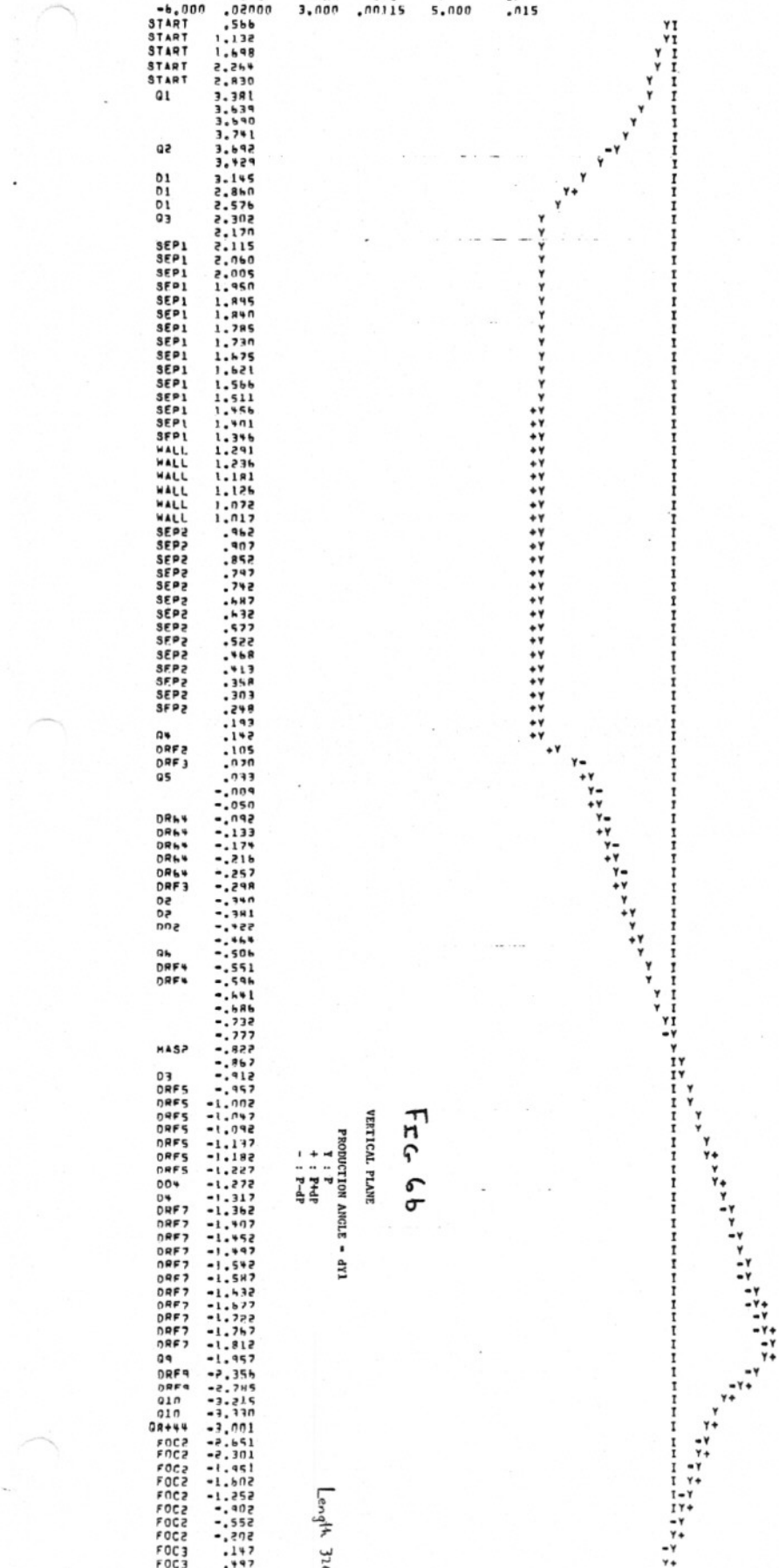

Fig 6b

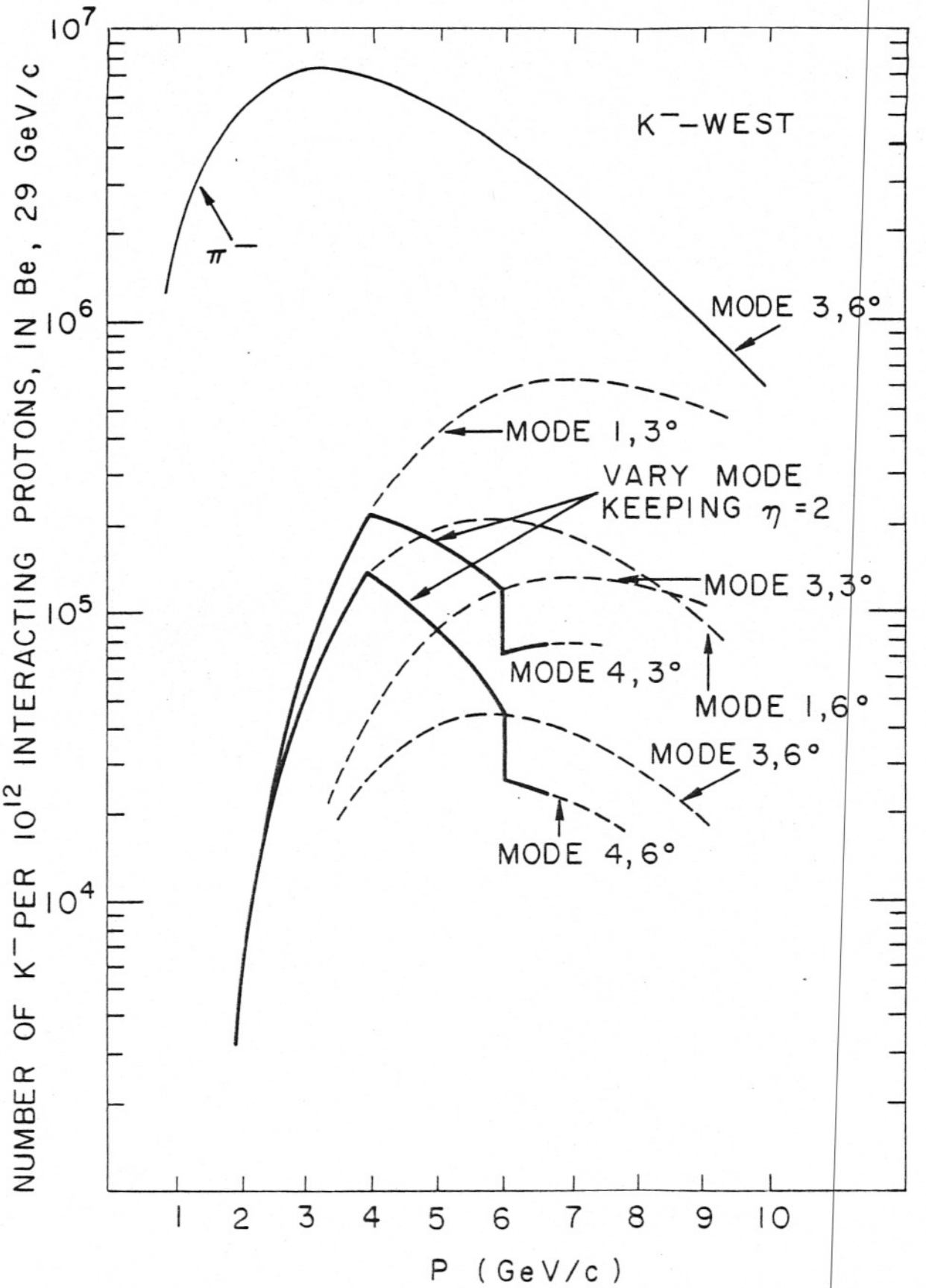
NUMBER OF K⁻ PER 10¹² INTERACTING PROTONS, IN Be, 29 GeV/c
10⁷
10⁶
10⁵
10⁴
K⁻-WEST
π⁻
MODE 3,6°
MODE 1,3°
VARY MODE
KEEPING η=2
MODE 3,3°
MODE 4,3°
MODE 1,6°
MODE 3,6°
MODE 4,6°
1 2 3 4 5 6 7 8 9 10
P (GeV/c)

Figure 8

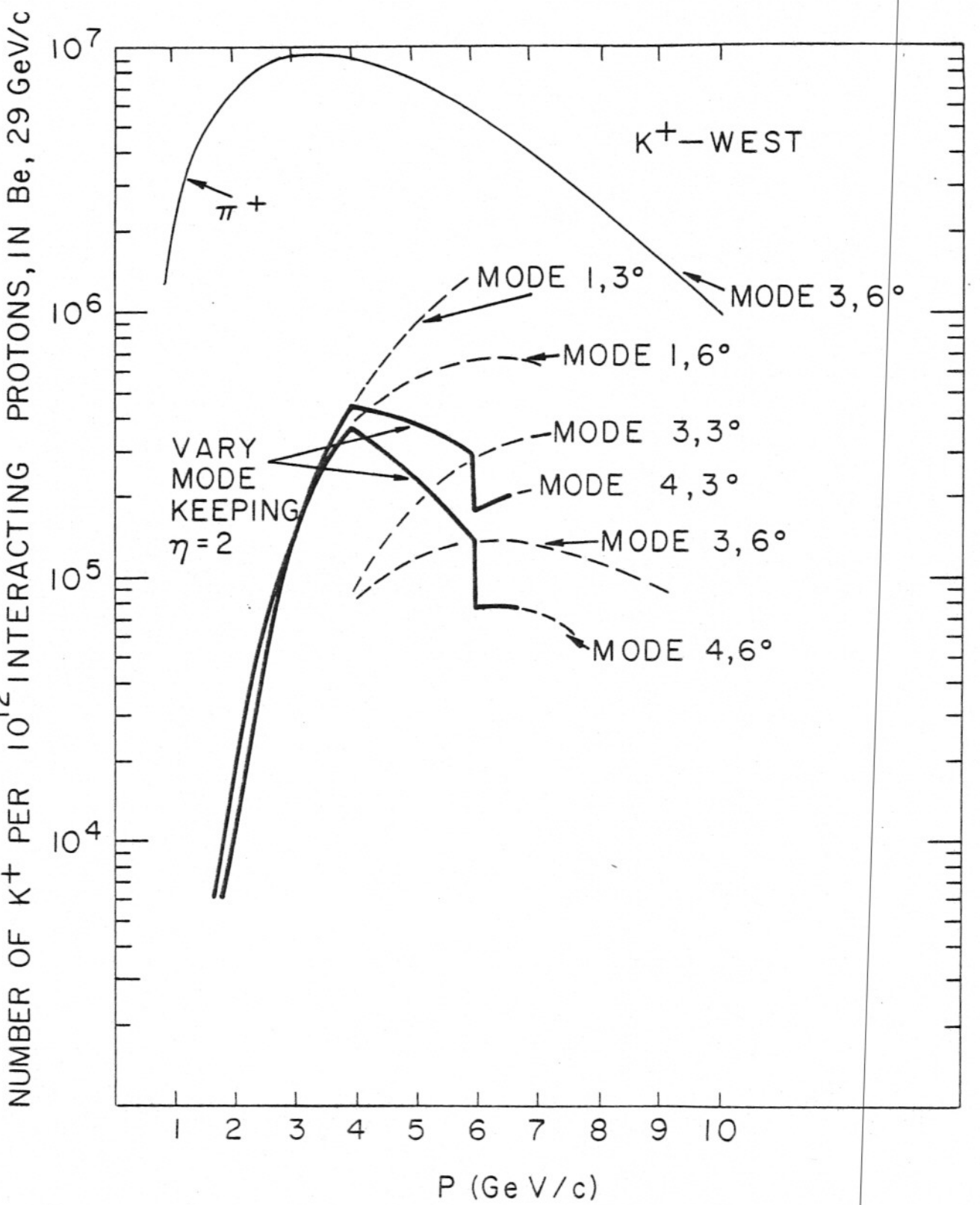
NUMBER OF K+ PER 10^12 INTERACTING PROTONS, IN Be, 29 GeV/c
10^7
10^6
10^5
10^4
K+—WEST
π+
MODE 1,3°
MODE 3,6°
MODE 1,6°
MODE 3,3°
MODE 4,3°
MODE 3,6°
MODE 4,6°
VARY
MODE
KEEPING
η=2
1 2 3 4 5 6 7 8 9 10
P (GeV/c)

Figure 9

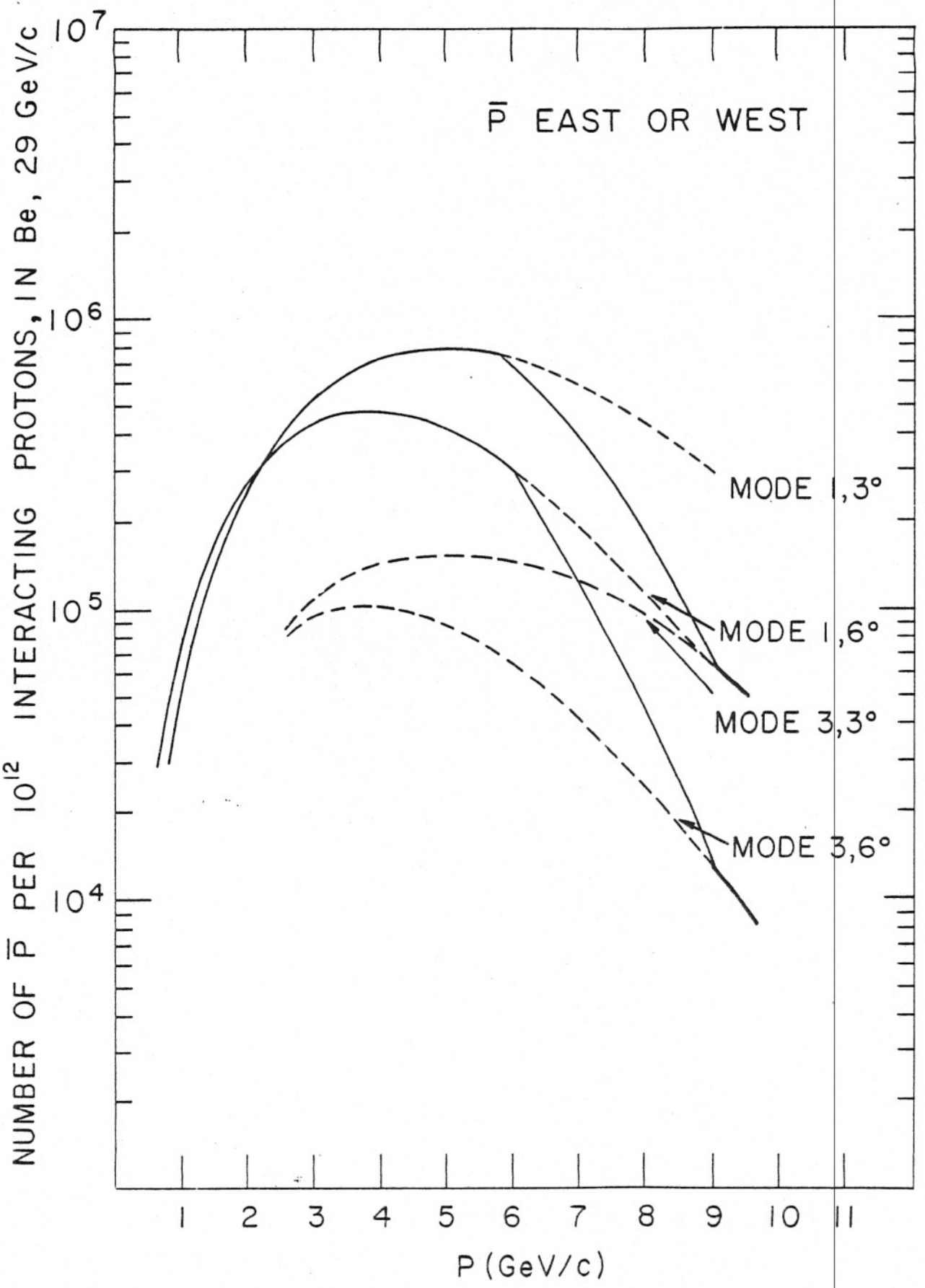
$\bar{P}$ EAST OR WEST
MODE 1,3°
MODE 1,6°
MODE 3,3°
MODE 3,6°
NUMBER OF $\bar{P}$ PER 10^{12} INTERACTING PROTONS, IN Be, 29 GeV/c
10^7
10^6
10^5
10^4
1 2 3 4 5 6 7 8 9 10 11
P (GeV/c)

Figure 10

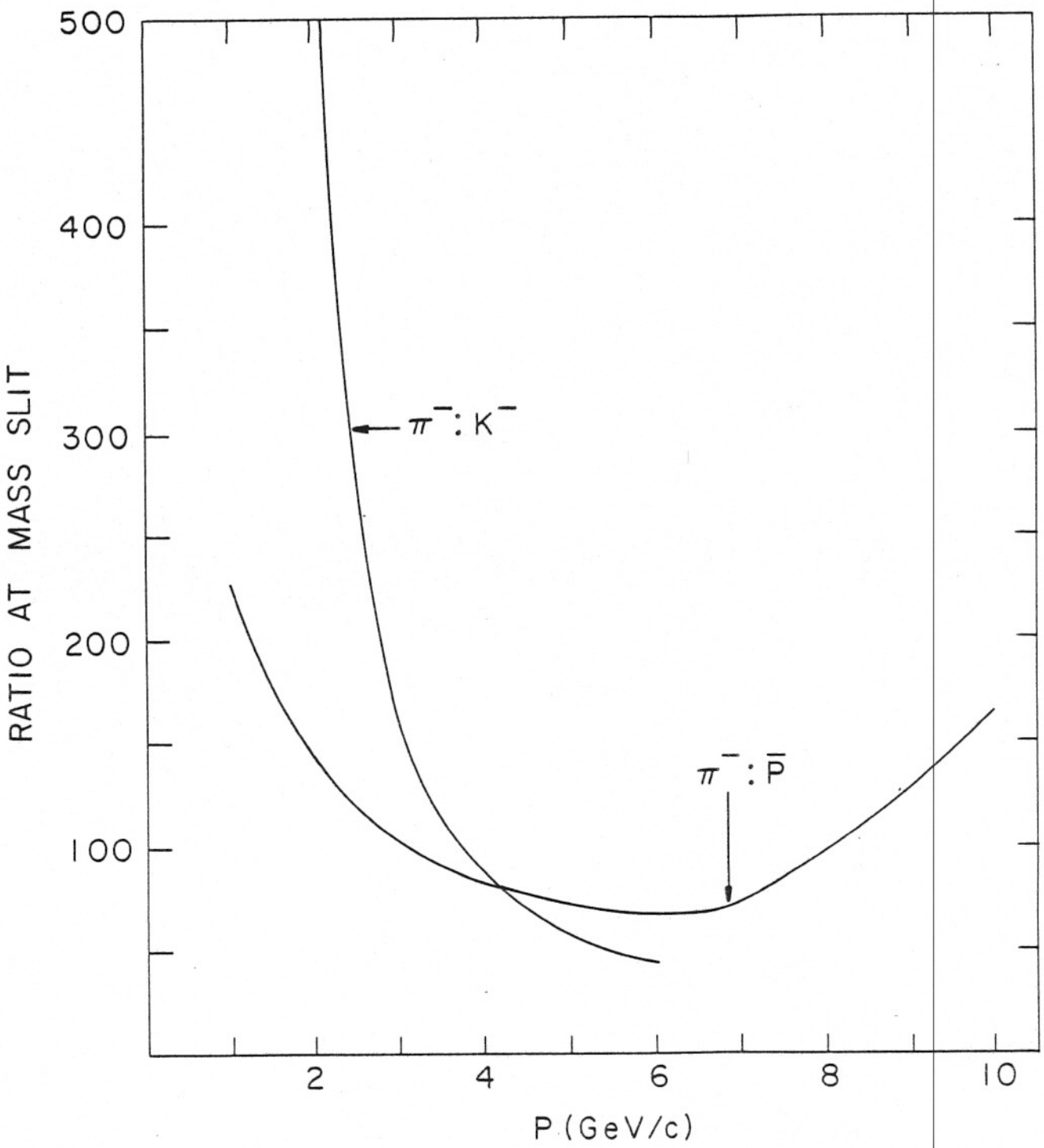
500
400
300
200
100
RATIO AT MASS SLIT
π^- : K^-
π^- : $\bar{P}$
2
4
6
8
10
P (GeV/c)

Figure 11

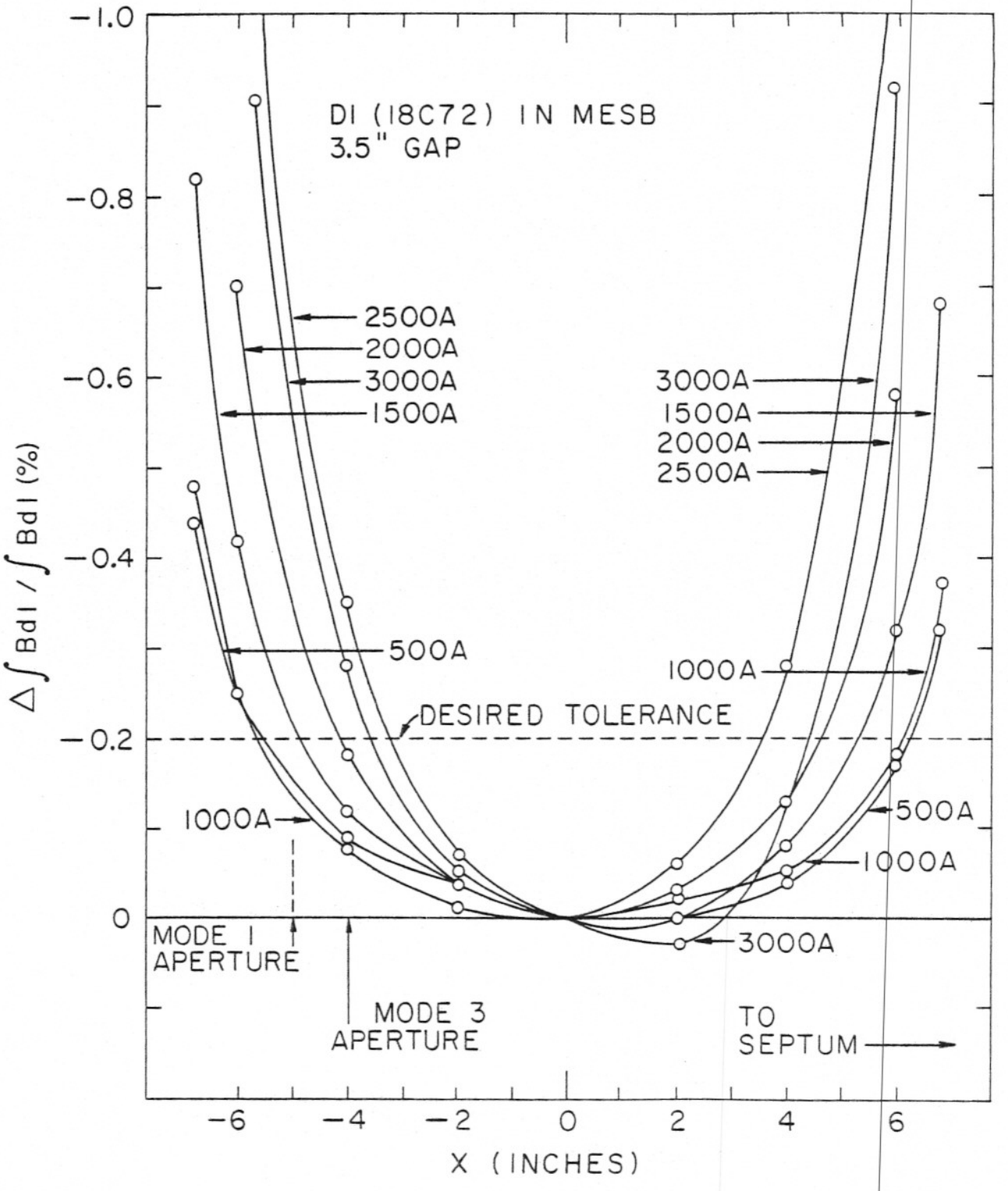
DI (18C72) IN MESB
3.5" GAP
2500A
2000A
3000A
1500A
500A
1000A
DESIRED TOLERANCE
3000A
1500A
2000A
2500A
1000A
500A
1000A
3000A
MODE 1
APERTURE
MODE 3
APERTURE
TO
SEPTUM
−1.0
−0.8
−0.6
−0.4
−0.2
0
−6
−4
−2
0
2
4
6
X (INCHES)
Δ∫BdI / ∫BdI (%)

Figure 12

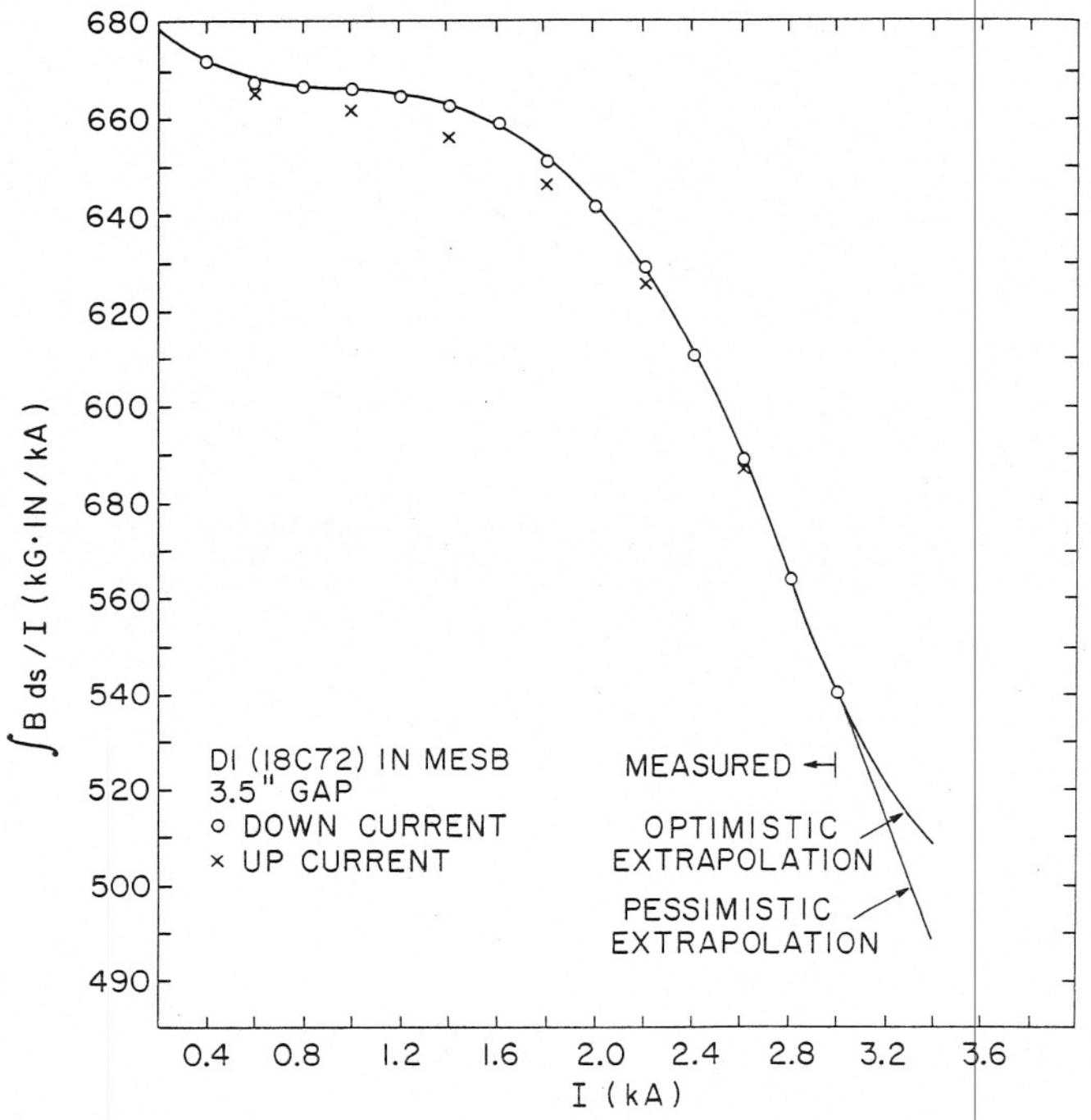
680
660
640
620
600
580
560
540
520
500
490
∫B ds / I (kG·IN / kA)
0.4
0.8
1.2
1.6
2.0
2.4
2.8
3.2
3.6
I (kA)
DI (18C72) IN MESB
3.5" GAP
o DOWN CURRENT
× UP CURRENT
MEASURED
OPTIMISTIC
EXTRAPOLATION
PESSIMISTIC
EXTRAPOLATION

Figure 13

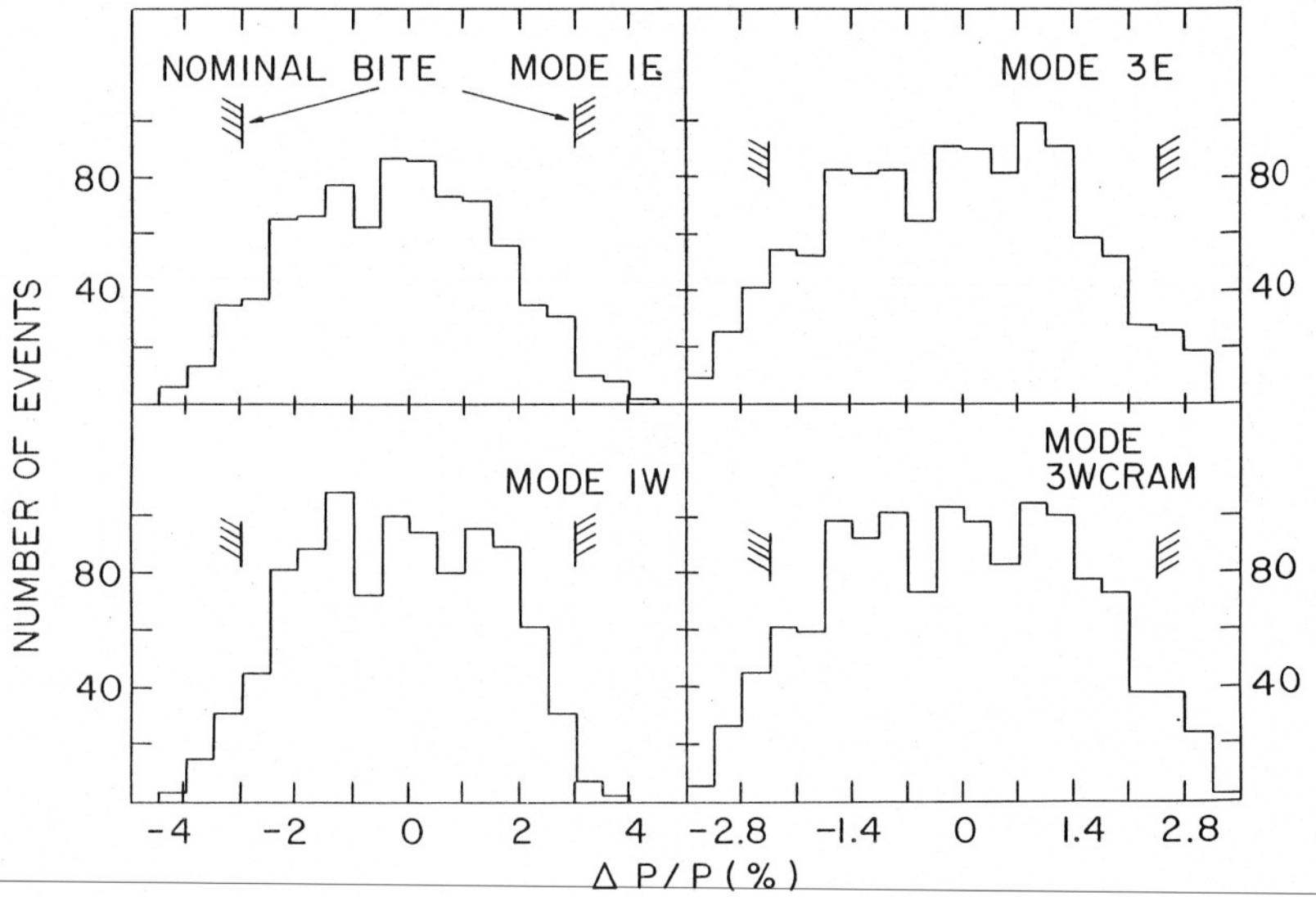
NOMINAL BITE
MODE IE
MODE 3E
MODE IW
MODE 3WCRAM
NUMBER OF EVENTS
80
40
-4
-2
0
2
4
-2.8
-1.4
0
1.4
2.8
Δ P/P (%)

Figure 14

The beam is of conventional design. Particles produced at 0° are focused by a doublet and momentum dispersed at slit located at the approximate mid-point of the channel. The second half of the beam is almost a reflection of the first; momenta are re-combined, and a second doublet brings the particles to their final focus.

Five quadrupoles form the upstream doublet. First, three N8Q32s focus vertically, then two 8Q48s horizontally. The beam is momentum dispersed at a slit located 700" from the production target by a 4.1^{o} bend in two 18D72s. The second bend is also 4.1^{o} in two 18D72s, and the second doublet consists of two 12Q60s focusing horizontally, then two vertically.

There are two collimators in the beam. B1C1 lies ahead of the first dipole and intercepts the diffracted protons. When narrowed, the slit walls can produce secondary particles, so this collimator cannot be used as an effective intensity limiter. B1C2 (the momentum slit) has remotely controlled horizontal and verticle appertures.

The beam has performed close to its design criteria. Table I gives some of its parameters, and Table II gives the currents, shunt readings, and Dybbuk set points for 20 GeV/c. Other operating points can be obtained by scaling.

Table I Beam Parameters

Vertical Acceptance	±16 mrad
Horizontal Acceptance	±4.8 mrad
Magnification at 2nd Focus	1.5 (V) x 1.3 (H)
Dispersion at Momentum Slit	1.6%/inch

Table II

B1 - 20 GeV/c Negative Beam

	Type	Current (Polarity)	Field or Gradient	Dybbuk
Q1	N8Q32	1913 (A)	2.225	1913
Q2	N8Q32	1913 (A)	2.225	1913
Q3	N8Q32	1913 (A)	2.225	1913
Q4	8Q48	1304 (B)	1.683	2086
Q5	8Q48	1304 (B)	1.683	2086
D1	18D72	1508 (B)	13.91	1508
D2	18D72	1508 (B)	13.91	1508
D3	18D72	1508 (B)	13.91	1508
D4	18D72	1508 (B)	13.91	1508
Q6	12Q60	995 (B)	0.830	1592
Q7	12Q60	995 (B)	0.830	1592
Q8	12Q60	961 (A)	0.803	1538
Q9	12Q60	961 (A)	0.803	961

Note: Dybbuk set points do not necessarily correspond to currents.